Appendix G: Development of Final A-Fault Rupture Models for WGCEP/ NSHMP Earthquake Rate Model 2

By Edward H. Field[1], Ray J. Weldon II[2], Thomas Parsons[3], Chris J. Wills[4], Timothy E. Dawson[3], Ross S. Stein[3], and Mark D. Petersen[5]

Open-File Report 2007-1437G

Version 1.0

2008

U.S. Department of the Interior
U.S. Geological Survey

[1]U.S. Geological Survey, Pasadena, California
[2]University of Oregon, Eugene
[3]U.S. Geological Survey, Menlo Park, California
[4]California Geological Survey, Sacramento, California
[5]U.S. Geological Survey, Golden, Colorado

U.S. Department of the Interior
DIRK KEMPTHORNE, Secretary

U.S. Geological Survey
Mark D. Myers, Director

U.S. Geological Survey, Reston, Virginia 2008

For product and ordering information:
World Wide Web: http://www.usgs.gov/pubprod
Telephone: 1-888-ASK-USGS

For more information on the USGS—the Federal source for science about the Earth, its natural and living resources, natural hazards, and the environment: World Wide Web: http://www.usgs.gov
Telephone: 1-888-ASK-USGS

Suggested citation:
Field, E.H., Weldon, R.J., II, Parsons, T., Wills, C.J., Dawson, T.E., Stein, R.S., and Petersen, M.D., 2008, Development of final A-Fault rupture models for WGCEP/NSHMP Earthquake Rate Model 2, *Appendix G in* The Uniform California Earthquake Rupture Forecast, version 2 (UCERF 2): U.S. Geological Survey Open-File Report 2007-1437G, 59 p. [http://pubs.usgs.gov/of/2007/1437/g/].

Contents

Introduction 1
Segmentation-Based Models 1
The General Solution 1
The Need for A-Priori Models: 4
Alternative Segment Slip Models: 5
Model Implementation and Parameter Sensitivity 7
Weighted Inversion: 8
A-Priori Models (and More on Segment Event-Rate Data): 9
Minimum Rate Constraints: 11
Slip Model, and Magnitude-Area Relationship: 11
Slip-Rate Reduction: 12
Mean Mag Correction: 13
Deformation Model: 13
Rupture Magnitude Frequency Distributions: 14
Final Chosen Solutions 14
Elsinore Fault: 15
Garlock Fault: 16
San Jacinto Fault: 16
Southern San Andreas Fault: 16
Northern San Andreas Fault: 17
Hayward-Rodgers Creek Fault: 17
Calaveras Fault: 18
Unsegmented Models 18
Results and Implications 19
Comparison with WGCEP UCERF 1 19
Future Improvements 20
References 20

Appendix G

Development of Final A-Fault Rupture Models for WGCEP/NSHMP Earthquake Rate Model 2

Edward Field, Ray Weldon, Vipin Gupta, Thomas Parsons, Chris Wills, Timothy Dawson, Ross Stein, and Mark Petersen

Introduction

This appendix discusses how we compute the magnitude and rate of earthquake ruptures for the seven Type-A faults (Elsinore, Garlock, San Jacinto, S. San Andreas, N. San Andreas, Hayward-Rodgers Creek, and Calaveras) in the WGCEP/NSHMP Earthquake Rate Model 2 (referred to as ERM 2. hereafter). By definition, Type-A faults are those that have relatively abundant paleoseismic information (*e.g.*, mean recurrence-interval estimates). The first section below discusses segmentation-based models, where ruptures are assumed be confined to one or more identifiable segments. The second section discusses an un-segmented-model option, the third section discusses results and implications, and we end with a discussion of possible future improvements. General background information can be found in the main report.

Segmentation-Based Models

Every previous WGCEP assumed segmentation in their models (although WGCEP-2002 also included some "floating" earthquakes over a narrow range of magnitudes). A fault segment is defined as one *or more* fault sections (from a given Deformation Model) that are assumed to rupture together and entirely during an earthquake. A rupture might involve one or more neighboring segments, but never involves only part of any segment (according to this model). Our goal is to determine the magnitude and long-term rate of every single and multi-segment-rupture combination on a given fault. We start here with a discussion of the general solution to this problem, then discuss the current implementation and parameter sensitivity, and finish with the final segmented-model solutions adopted by the present WGCEP.

The General Solution

If there are S fault segments (with no branches), then there are $R=S(S+1)/2$ different ruptures involving contiguous segments (*e.g.*, Figure 1). Our goal is to determine the long-term rate (f_r) of each r^{th} rupture. The potential data constraints we have to work with are:

- Long-term slip rates of each segment (v_s)
- The mean total rate of events on each segment (λ_s), which can also be stated as one over the mean recurrence interval (MRI) of each segment.
- A-priori information on the rate of the r^{th} rupture ($f_r^{a-priori}$). An example would be the historical rate of Parkfield segment ruptures. Another would be setting a single-segment rate to zero because repeated large-slip offsets there imply that it's highly unlikely to go by itself.

These constraints can be written as:

$$\sum_{r=1}^{R} D_{sr} f_r = v_s \qquad \text{Equation Set (1)}$$

$$\sum_{r=1}^{R} G_{sr} f_r = \lambda_s \qquad \text{Equation Set (2)}$$

$$f_r = f_r^{a-priori} \qquad \text{Equation Set (3)}$$

where D_{sr} is the average slip in the r^{th} rupture on the s^{th} segment, and G_{sr} is a matrix indicating whether the r^{th} rupture involves the s^{th} segment (1.0 if so, 0.0 if not).

Equation Set (1) is simply an expression of moment balance. It gives S equations for the R unknowns (generally all these equations will be available because slip-rate estimates are available for all type-A fault segments). Equation Set (2) gives up to S equations for the R unknowns depending on whether independent segment-rate data are available (by independent we mean the segment rates are not simply computed from the slip-rate and displacement data used in Equation Set (1)). Equation Set (2) appears to double the number of equations compared to Equation Set (1), thereby increasing the likelihood of finding a unique solution (more toward an over-determined system of equations). However, these equations are unique only to the extent D_{sr} really depends on r. For example, if we take the "Characteristic Slip" assumption that $D_{sr} = D_s$ (average slip per event is independent of whether it's a single or multi-segment rupture), then we can divide both sides of Equation Set (1) by D_s to see that the equations are identical to Equation Set (2) (because $\lambda_s = v_s / D_s$ under the "Characteristic Slip" assumption). Nevertheless, Equation Set (2) will help constrain the solution space to the extent D_{sr} actually depends on r.

The above set of equations can easily be solved in the least-squares sense using standard linear inverse theory (*e.g.*, Menke, 1989). Specifically, if we combine all available equations into one system as:

$$\boldsymbol{Xf} = \boldsymbol{d}$$

where $\boldsymbol{f}$ is a vector of rupture rates that we wish to solve for, and $\boldsymbol{d}$ is a vector of data constraints, then the minimum-length solution is simply that which minimizes the total prediction error (defined as the sum of the squares of the differences between the observed and predicted data):

$$E = \sum \left(d_i^{obs} - d_i^{pre} \right)^2 = (\, \boldsymbol{d} - \boldsymbol{Xf})^{\mathrm{T}} \, (\, \boldsymbol{d} - \boldsymbol{Xf}).$$

where i corresponds to the ith segment or rupture (depending on the type of constraint). If we have uncertainty estimates for all data (σ_{d_i}), then we can solve for the weighted least squares solution by minimizing:

$$E = \sum \left[\frac{\left(d_i^{obs} - d_i^{pre} \right)}{\sigma_{d_i}} \right]^2 = (\, \boldsymbol{d} - \boldsymbol{Xf})^{\mathrm{T}} \, \boldsymbol{W} \, (\, \boldsymbol{d} - \boldsymbol{Xf}) \qquad (4)$$

where $\boldsymbol{W}$ is a diagonal matrix of weights ($1/\sigma_{d_i}^2$). In the discussion below, we will refer to the term in brackets ($\left(d_i^{obs} - d_i^{pre}\right)/\sigma_{d_i}$) as the "normalized residual", and the total sum (E) as the "generalized prediction error". It may sometimes be useful to separate E into contributions from the different equations sets above:

Slip-Rate Prediction Error:
$$E_v = \sum \left[\frac{\left(v_s^{obs} - v_s^{pre}\right)}{\sigma_{v_s}} \right]^2$$

Segment Event-Rate Prediction Error:
$$E_\lambda = \sum \left[\frac{\left(\lambda_s^{obs} - \lambda_s^{pre}\right)}{\sigma_{\lambda_s}} \right]^2$$

A-Priori Model Prediction Error:
$$E_{a-priori} = \sum \left[\frac{\left(f_r^{a-priori} - f_r^{pre}\right)}{\sigma_{a-priori_r}} \right]^2$$

where

$$E = E_v + E_\lambda + E_{a-priori}$$

It is important to keep in mind that the weighted least squares solution assumes data uncertainties are adequately approximated by a Gaussian distribution, uncorrelated, and precisely known (or at least the relative uncertainties are precisely known).

Because rates cannot be negative, an important additional constraint is positivity:

$$f_r \geq 0,$$

While this is helpful in terms of further narrowing the solution space, it makes finding and understanding the inverse solution more difficult (*e.g.*, Singular Value Decomposition cannot be used). We use the Non-Negative Least Squares (NNLS) solution of Lawson and Hanson (1974). The weighted inversion is obtained by multiplying both sides of each equation by $1/\sigma_i$ before solving the NNLS problem. Note that the positivity constraint on f_r, and v_s and λ_s for that matter, is an explicit violation of the presumed Gaussian statistics; we proceed nonetheless.

Finally, it may be desirable to force final rupture rates to be greater than some specified minimum values ($f_r \geq f_r^{min}$). Putting these values into a vector $\boldsymbol{f^{min}}$, we achieve this constraint by defining

$$\boldsymbol{f' = f - f^{min}}$$

and

$$\boldsymbol{d' = d - X f^{min}},$$

and then solving

$$\boldsymbol{X f' = d'}$$

for $\boldsymbol{f'}$ using NNLS, and then obtaining the final solution as

$$\boldsymbol{f} = \boldsymbol{f'} + \boldsymbol{f}^{\boldsymbol{min}}.$$

The Need for A-Priori Models:

In most circumstances applying Equation Set (1) and perhaps (2) leads to an underdetermined system of equations, meaning an infinite number of solutions exist. For example, consider Equations Set (1) for a two-segment/three-ruptures case:

$$D_{11}f_1 + 0f_2 + D_{13}f_3 = v_1$$
$$0f_1 + D_{22}f_2 + D_{23}f_3 = v_2$$

(where rupture 1 involves only segment 1, rupture 2 involves only segment 2, and rupture 3 involves both segments. This equation set has only two equations for three unknowns, meaning it is underdetermined, To see the implications, we can solve for f_2 and f_3 in terms of f_1 as:

$$f_3 = (v_1 - D_{11}f_1)/D_{13}$$
$$f_2 = [v_2 - D_{23}f_3]/D_{22} = [v_2/D_{23} - v_1/D_{13} + D_{11}f_1/D_{13}]D_{23}/D_{22}$$

In this case f_1 can take on any value between v_1/D_{11} (if f_3 = 0) and 0 (if $f_3 = v_1/D_{13}$ and $v_1/D_{13} < v_2/D_{23}$ to prevent f_2 from being negative). This continuum of possible values for f_1 means there are an infinite number of solutions. Adding mean-segment-rate data (λ_s) via Equation Set (2) may help define a unique solution. However, if there are more than three segments on the fault, then the number of equations represented by Equation Set (1) and (2) will always be less than the number of ruptures (unknowns).

One way to solve the system of equations, that which will be pursued here, is to define a complete set of a-priori rates ($\boldsymbol{f}^{\boldsymbol{a\text{-}priori}}$) representing an initial estimate or guess. The final, post-inversion solution will then be that which is as close as possible to all the data, including this initial guess, in a weighted least-squares sense. Of course this doesn't really solve the non-uniqueness problem, as we are still left with choosing among an infinite range of alternative initial guesses. We therefore need a well-defined, rational scheme for obtaining a finite number of solutions. The range of viable solutions represents an epistemic uncertainty in that at most, only one model can be the correct long-term behavior of the fault (assuming the correctness of the basic segmentation assumption).

From the perspective of SHA, we want to obtain a range of models that span the hazard implications. To this end, we can define the following alternative a-priori solutions:

- Geological Insight Solution - A best estimate based on considering all available historic and paleoseismic constraints (*e.g.*, the extent to which dates of events on neighboring segments do or do not overlap).

- Minimum Rate Solution - An end-member model that minimizes the total rate of ruptures (and therefore maximizes event magnitudes), while honoring the data. This would be the f_1=0 and f_2=0 case in our 2-segment example above (assuming the historic or paleoseismic record does not stipulate otherwise).
- Maximum Rate Solution - An end-member model that maximizes the total rate of ruptures (and therefore minimizes event magnitudes), while honoring the data. This would be the $f_3 = 0$ case in our 2-segment example above (assuming the historic or paleoseismic record does not stipulate otherwise).

For a given set of assumptions (*e.g.*, segment-slip and magnitude-area models described below) each of these a-priori models yields a unique post-inversion model. Additional models can obviously be constructed as a weighted combination of these three results. However, not all viable models can be constructed from such a linear combination because these solutions do not, in general, span the solution space. It might be valid to presume, however, that these models adequately span the range or hazard and/or loss. Furthermore, additional geologic insight models can be defined if a more thorough exploration of the solution space is desired.

The development of the three a-priori models for each fault is described elsewhere (i.e., Appendix E for the southern San Andreas fault; Appendix F for the San Jacinto, Garlock, and Whittier-Elsinore faults; and in Appendix K for Type-A faults in northern California, where these models represent WGCEP-2002 average rates with some slight modifications to be consistent with more recent paleoseismic data). In general, these a-priori solutions were developed "by hand" by partitioning the number of events in a given period of time among the various rupture options, while considering all available information. The resultant models generally match mean segment recurrence interval data explicitly where available. However, depending on the assumed slip on each segment for each rupture (D_{sr}, discussed more below) these a-priori models may or may not be moment-rate balanced in terms of honoring Equation Set (1). This is where the inversion comes in. Specifically, we find a final, unique solution that is as close as possible, in a least squares sense, to the a-prior rupture rates in Equation Set (3), while also satisfying the slip-rate and segment-rate data in Equations Sets (1) and (2).

Alternative Segment Slip Models:

One needs to know the average slip on each segment in each rupture (D_{sr}) in order to solve Equation Set (1). We consider the following four alternative models:

1. *Characteristic Slip* ($D_{sr} = D_s$)
2. *WGCEP-2002 Model* ($D_{sr} \propto v_s$)
3. *Uniform/Boxcar Slip* ($D_{sr} = D_r$)
4. *Tapered Ends* ($[Sin\ (x)]^{0.5}$)

The "*Characteristic Slip*" model was adopted by the 1995 WGCEP for their Type A Faults. This model assumes that the average slip on a segment is independent of whether the segment ruptures alone or simultaneously with neighboring segments:

$$D_{sr} = D_s = v_s / \lambda_s$$

As mentioned above, under this assumption Equation Sets (1) and (2) are identical, making the solution space even less determined (more non-unique). However, this assumption does make it relatively simple to "hand build" moment-balanced solutions (i.e., because Equations Set (1) simplifies to Equation Set (2)).

Note that a magnitude-area relationship is not needed for this model because rupture moment is computed from:

$$Mo_r = \mu \sum_{s=1}^{S} (G_{sr} A_s D_s) = \mu \sum_{s=1}^{S} (G_{sr} A_s v_s / \lambda_s) \quad (5)$$

where A_s is segment area and μ is the shear modulus (assumed to be equal to 3e10 N-m), and magnitude is computed from the moment-magnitude relationship:

$$M_r = \frac{\log(Mo_r) - 9.05}{1.5} \quad (6)$$

(Hanks and Kanamori, 1979). In fact, one way to check this model is to see how the implied magnitudes and areas of the ruptures compare to the various viable magnitude-area relationships (discussed below in the context of Figure 7).

The "*WGCEP-2002 Slip*" model is that implied by how the WGCEP (2002) constructed their rupture models. Their overall approach was to define various scenarios, where each scenario was a set of earthquakes such that each segment ruptured exactly once in a given fault cycle (see Figure 1). For example, one end-member scenario is where all segment rupture independently, and another scenario is where they all rupture together. Models were constructed as a weighted average of the various possible scenarios, where the weights were based on the following question posed to participants: "If the entire length of a fault failed completely 100 times, what would be the frequency (percentage) of each rupture scenario?" (WGCEP, 2002, page 3.3). This procedure does not necessarily produce a moment-balanced model, so their Fortran code solved for the nearest set of weights that is moment balanced (i.e., where the weights represent the fraction of total moment put into each scenario).

The magnitude for each rupture is obtained from a magnitude-area relationship ($M_r = M(A_r)$, where A_r is total rupture area), which consequently defines the average slip for each rupture from the moment-magnitude relationship:

$$D_r = \frac{10^{1.5 M_r + 9.05}}{\mu A_r}$$

where μ is taken as 3e10 N-m. The average slip on each segment of a multi-segment rupture is not the same in this model, however, but is proportional to the slip rate in each segment:

$$D_{sr} = D_r \frac{v_s A_r}{\sum G_{sr} v_s A_s}$$

The need for this slip distribution can be understood by considering the case where all moment rate is put into the one scenario where all segments always rupture together (only full-fault events); because the slip rate in each segment is the product of the rate of the rupture and the average slip on the segment, the average slip on each segment must vary according to the slip rate because the event rate is constant. Given this presumed slip distribution, each of their scenarios represents a solution to Equation Set (1). In fact, their scenarios span the solution space under this slip-distribution assumption (all solutions can be expressed as a weighted sum of their scenarios).

Note that our inversion scheme outlined above represents a generalization of the WGCEP-2002 approach, with their particular procedure being one of several options. More specifically, their voting on alternative scenarios was essentially a process of defining geologic-insight a-priori models. Furthermore, the regression in their Fortran code to find the closest moment-balanced model was effectively a simplification of our inversion made possible by their particular slip-distribution assumption (and by their exclusion of Equation Set (2), as they did not apply any segment event-rate constraints, but rather used these as a consistency check with the final results).

The ongoing WGCEP found two troubling aspects of the WGCEP-2002 slip model: 1) a lack of observational evidence that slip on a segment is proportional to slip rate; and 2) that the resultant solution space precludes some desired solutions. An example of the latter that came up during current WGCEP deliberations is as follows: if one stipulates that one segment can only rupture in full-fault events (*e.g.*, because the mean recurrence interval and/or observed slip per event is quite high), then all other segments can only rupture as full-fault events as well (which may be inconsistent with recurrence intervals or slip observed on other segments). Another example is if a segment at the end of the fault can never go alone, then neither can the adjacent segment ever go alone (as can been seen from examination of Figure 1). These restrictions are a manifestation of the assumed slip on each segment in multi-segment ruptures. In spite of these limitations, this solution is kept as a viable option by the current WGCEP (*e.g.*, because it's that only model that can allow having *only* full-fault ruptures while satisfying slip rates that vary among segments).

The "*Uniform/Boxcar Slip*" model assumes that the average slip on all segments is the same within a given rupture ($(D_{sr} = D_r)$), where D_r is obtained from a magnitude-area relationship as in the WGCEP-2002 Slip model. Finally, the "*Tapered Ends Slip*" model assumes that, on average, the slip at a point x along rupture is:

$$D(x) \propto \sqrt{Sin(x\pi)} \qquad 0 \bullet x \bullet 1$$

This functional form was found to be the best fit to an average of 13 historical events (Figure 10 of Appendix E). D_{sr} is obtained by averaging this function over the length of each segment, where the total average slip is again constrained by a magnitude-area relationship.

Model Implementation and Parameter Sensitivity

In this section we describe the current model implementation and explore implications of various alternative parameter settings (logic tree branches). The adjustable parameters relevant to the segmented A-fault rupture models are listed in Table 1 along with a brief description of each (more details are discussed below as needed in the context of presenting results). Given the number of alternative settings for each parameter, there are hundreds to thousands of possible logic-tree branches (depending on how densely the alternatives are sampled). Consequently, our

exploration of parameter space here will be limited, but nevertheless hopefully illustrative. There are a total 123 different possible ruptures given the seven Type-A faults. Listing pertinent information for each (magnitude, rate, etc.) for even a single set of parameters would take about four text pages using small font. In lieu of such clutter, we make reference to some html-linked Excel spreadsheets. Those not interested in such details can skip to the "Final Chosen Solutions" section below (where numerical values are listed explicitly).

All of the figures and tables that follow were generated using a custom, *OpenSHA*-based graphical user interface to the model available at:

http://www.WGCEP.org/resources/tools/UCERF2_GUI.html

This application can be used to explore options and results that go way beyond what we are able to present here.

The segment data needed to implement the models for the seven Type A faults are listed in Table 2 (see caption for some important details). In the discussions that follow, default parameter settings (listed in bold typeface in Table 1) have been applied unless otherwise noted.

Weighted Inversion:

The following three adjustable parameters influence how the equations are weighted in the inversion:

Wt On A-Priori Rates
Relative Wt On Segment Rates
Weighted Inversion?

If "*Weighted Inversion?*" is *true*, then the slip-rate and segment-event-rate uncertainties listed in Table 2 are used as weights in the inversion (i.e., in minimizing equation 4). If the value is *false*, then all data uncertainties are effectively equal to 1.0. Histograms of normalized residuals for slip-rate and event-rate data are shown in Figure 2 for the *true* case (the default value), and in Figure 3 for the *false* case (note that some parameters have been changed from their default values for this comparison; see figure captions for details). As expected, "*Weighted Inversion?*" = *true* provides a better fit to the data in terms of normalized residuals, although the effect is not dramatic.

The "*Relative Wt On Segment Rates*" parameter provides a relative weighting for the segment event-rate data with respect to the slip-rate data. Values increasingly greater than 1.0 favor fitting the event-rate data more, and values less than 1.0 favor fitting the slip rate data more. A value of zero means Equation Set (2) is excluded altogether, the result of which is shown in Figure 4. In general a value of zero should produce a perfect fit to all slip-rate data; the non-zero residuals seen in Figure 4 result from a constraint that has been placed on the rate of single-segment ruptures of the "Clark" segment of the San Jacinto Fault (discussed more below). As shown in Figure 5, very high values of "*Relative Wt On Segment Rates*" produce a perfect fit to the event-rate data, but at the cost of some rather high residuals on the slip rate data.

"*Wt On A-Priori Rates*" specifies how well the a-prior rates are to be matched. More specifically, the value entered is defined as

$$Wt\ On\ A\text{-}Priori\ Rates = f_r^{a-priori} \Big/ \sigma_{a-priori_r} \quad (7)$$

for use in the weighted inversion (minimization of equation (4)). Thus, the actual weight applied is:

$$1/\sigma_{a-priori_r} = Wt\ On\ A\text{-}Priori\ Rates\ \ / f_r^{a-priori} \quad (8)$$

The normalization by $f_r^{a-priori}$ in equation (8) serves to equalize the influence of each *a priori* rupture rate (otherwise higher-rate ruptures would have a disproportionate influence on the inversion, which was found to be problematic in earlier versions of the model). If $f_r^{a-priori}$ is zero, then the least non-zero value of $f_r^{a-priori}$ for the fault as a whole is applied (to avoid infinite weight). A value of zero for "*Wt On A-Priori Rates"* means Equation Set (3) is excluded completely from the inversion, and increasingly large values mean the a-priori rates are matched better and better (at the cost of a poorer fit to the segment slip-rate and event-rate data). A thorough sensitivity analysis with respect to this parameter, with all other parameters being set to default values, revealed the following behavior: values less than 1e-16 are equivalent to leaving Equation Set (3) out of the inversion (they have the same generalized prediction error); values between 1e-13 and 1e-2 represent a "stable zone" in that the exact same solution is obtained (with the same generalized prediction error); values increasing from 1e-2 cause the a-priori rates to be matched better and better; and all values above 1e4 cause the a-priori rates to be matched exactly (with the same generalized prediction error). The "stable zone" referred to above (that is, "*Wt On A-Priori Rates*" values between 1e-13 and 1e-2) is interpreted as the solution that represents a best fit to the segment slip-rate and/or event-rate data, but that is also as close as possible to the a-priori model. In other words, this allows the final solution to wander away from the a-priori rates as much as needed to match the slip-rate and/or event-rate data (in a least-squares sense), but no further. This is precisely what was done in the WGCEP-2002 Fortran code (for a more limited set of options than presented here). The default value of 1e-4 was chosen because it is in the stable zone, with respect to all the a-priori models, slip-distribution models, and magnitude-area relationships.

A-Priori Models (and More on Segment Event-Rate Data):

The "*Segmented A-Fault Solution Types*" parameter allows one to select the a-priori model. As discussed above, *Minimum Rate*, *Maximum Rate*, and *Geologic Insight* a-priori models were developed for each fault (the latter being the default/preferred value). The rupture rates for each are listed on the summary sheet of the Excel file:

http://www.WGCEP.org/resources/documents/UCERF2_FinalReport/A_Faults_aPrioriRates.xls

Rates for the geologic-insight a-priori models are also listed in Table 3 here.

Interestingly, if the value of *Relative Wt On Segment Rates* = 1.0 (meaning include the data with a weight generally equal to slip-rate data) then the *Minimum Rate*, *Maximum Rate*, and *Geologic Insight* a-priori models all converge to the same final rates on some faults that have event-rate data on the majority of segments (*e.g.*, Elsinore). This indicates that recurrence-interval data have a very powerful influence on the inversion, and in particular, that the problem is over-determined at least in the neighborhood of the a-priori models.

If we had confidence that our segment event-rate data were reliable, the convergence of the *Minimum Rate*, *Maximum Rate*, and "*Geologic Insight*" models would be good news (effectively eliminating a branch of the logic tree). However, and as discussed extensively in Appendix C, the segment event-rate data are not generally well determined (*e.g.*, different estimates are obtained whether you assume the underlying distribution of inter-event times is Poissonian or Browning Passage Time). Even though we account for the uncertainties to some extent in the calculation (via the *Weighted Inversion?* parameter), the exact value of the "best-estimate" event rates nevertheless have a powerful influence. The better way to include segment event-rate data would be to form a logic-tree branch to account for alternative possible values (thereby leading to different post-inversion solutions). However, another important issue that has not been fully addressed is the influence of missed or extra events in the paleoseismic record (which could be biasing the event-rate estimates).

A final issue with respect to including segment event-rate data in the inversion is correlation with the a-priori constraints. As mentioned above, the a-priori models are generally constructed to match segment event-rates explicitly (but generally not slip-rate data because that depends on too many other parameters). Therefore, including both the a-priori models and segment event rates is in some sense double counting.

To avoid all these potential pitfalls, the current working group decided to use the segment event-rate data only as a reality check on post inversion results. In other words, we set "*Relative Wt On Segment Rates*" = 0 (the default value), but compare the post-inversion results to segment event-rate data to make sure the moment balancing (Equation Set (1)) has not introduced inconsistencies with event rate estimates.

Setting "*Relative Wt On Segment Rates*" = 0 means we are only including Equation Sets (1) and (3) in the inversion, and with *Wt On A-Priori Rates* = 1e-4 we are effectively finding the moment-balance model that is closest to the a-priori model. However, it's very important to understand that in our least-squares solution, "closest to" is defined as minimizing an L-2 norm (the prediction error in Equation (4)). This can lead to some potentially non-intuitive results, especially for the *Minimum*- and *Maximum-Rate* a-priori models. For example, the *Minimum Rate* a-priori models are generally defined to maximize the rate of the largest (full-fault) event. If the a-priori model under-predicts the total moment rate, then one would expect the inversion to simply increase the rate of that full-fault rupture. However, this can lead to a larger total prediction error (Equation (4)) than if some of the rates of smaller events are also increased, which means the latter will be given as the solution. Therefore, the post-inversion "minimum rate" model may not represent the moment-balanced model that has the lowest total rate of events (i.e., our L-2 norm minimization should not be confused with an L-1 norm minimization). While such effects are generally not dramatic, they should nevertheless be kept in mind. Another subtle issue that can influence inversion results, especially for the *Minimum*- and *Maximum-Rate* models, is exactly how zero a-priori rates are handled in setting weights (Equation (8)).

The bottom line is that inversion results need to be considered carefully for the *Minimum-Rate* and *Maximum-Rate* models, and we have not yet had the time to do so. Development of these end-member models has not been a high priority because they will presumably not influence the mean hazard and loss estimates being conducted by the NSHMP and CEA, respectively

Minimum Rate Constraints:

Recall that that our formulation allows one to define a minimum post-inversion rate for each rupture (f_r^{min}). One reason for setting these to values greater than zero would be to avoid saying anything can't happen. Furthermore, the rates for some events in the a-priori models are listed either as "Unknown" (meaning there is no supporting evidence for) or "Unlikely" (meaning there is evidence against); the rates for both these types are set to zero in Equation-Set (3). The "*Min Fraction for Unlikely Ruptures*" parameter specifies f_r^{min} for all events deemed unlikely in the a-priori model. More specifically, f_r^{min} for these unlikely events is defined as the value of "*Min Fraction for Unlikely Ruptures*" times the minimum rate of all events in the a-priori model (excluding the zero rate values assigned to the unlikely and unknown ruptures). The value of f_r^{min} for all other ruptures (both unknown and those with actual rates) is defined by the value of the "*Min Fraction for Unknown Ruptures*" parameter multiplied by the minimum rate in the a-priori model (again, ignoring the zero rate values assigned to the unlikely and unknown ruptures). This scheme implies that all f_r^{min} are set to zero if any rupture in the a-priori model has zero rate (ignoring those defined as unlikely or unknown).
The default values for "*Min Fraction for Unknown Ruptures*" and "*Min Fraction for Unlikely Ruptures*" are 0.5 and 0.1, respectively, when applying the geologic-insight a-priori models. "Unlikely" ruptures are those in which evidence exists suggesting they do not occur, and "unknown" ruptures are those for which no evidence was found for or against the rupture occurring. Assuming that the level of investigation is reasonably constant for an individual fault, we infer that the resolution threshold is approximately the least frequent rupture rate observed. It is assumed that it is as likely that an "unknown" rupture occurs at the threshold level (if it were above the threshold we would see it) or not at all, and thus an "unknown" rupture is assigned 0.5 the rate of the threshold (a 50-percent chance). "Unlikely" ruptures are assumed to be about an order of magnitude (0.1) less likely to occur than our observation threshold because the uncertainties in paleoseismic inference make it impossible to completely rule out a possible rupture. Thus, we give "unlikely" ruptures a minimal (i.e. an order of magnitude less, 0.1) value relative to our observation threshold.

The normalized residual for these default settings (and in fact, the case where all parameters are set to the defaults listed in Table 1) are shown in Figure 6. Note that enforcing these minima can produce an inability to fit some slip-rate data, which can be seen from the fact that Figure 6 has a few more non-zero slip-rate residuals than the case in Figure 4 (which is the same, except that these minima were set to zero).

Slip Model, and Magnitude-Area Relationship:

The "*A-Fault Slip Model*" parameter determines how the segment slip for each rupture (D_{sr}) is computed. The options already discussed are:

Characteristic Slip ($D_{sr} = D_s$)
WGCEP-2002 Model ($D_{sr} \propto v_s$)
Uniform/Boxcar Slip ($D_{sr} = D_r$)
Tapered Ends ($[Sin\ (x)]^{0.5}$)

If *Characteristic Slip* has not been chosen, then one needs to specify a magnitude-area relationship using the "*Mag-Area Relationship*" parameter. Base on the evaluation in Appendix D, the following options are supported:

Ellsworth-A (WGCEP, 2002, Eq 4.5a)
Ellsworth-B (WGCEP, 2002, Eq 4.5b)
Hanks & Bakun (2002)
Somerville (2006)

Figure 7 shows each of these magnitude-area relationships, along with the magnitude-area implications of the *Characteristic Slip* assumption for the fault models considered here (computed using equations (5) & (6)). There is a wide range of magnitudes for given area implied by the *Characteristic Slip* model, and this is before any aleatory variability for a given rupture magnitude has been added via the "*Mag Sigma*" and "*Truncation Level*" parameters discussed below. Adding the latter produces a total range of more than one magnitude unit for given area.

To explore the influence of these parameter options, the following Excel file gives the magnitude and post-inversion rate of each rupture for all combinations of "*A-Fault Slip Model*" and "*Mag-Area Relationship*" (all other parameters being set to default values; see the "README" sheet in the file for more info on how to interpret the results):

Test1_A_FaultRupRates.xls

(available from http://www.WGCEP.org/resources/documents/UCERF2_FinalReport)

The "Gen. Pred. Err." sheet in this Excel file lists the total generalized prediction errors (Equation (4)), giving an indication of how well each case fits the data (note that the computation of these total errors has included the event-rate data even though they were excluded from the inversion, and the misfit to the a-priori models has negligible influence given the low weight these are given). While it might be tempting to rank the various slip-model and magnitude-area relationship combinations according to the total prediction error, care must be taken because this error can be dominated by residuals on just a few segments (leading to conclusions that are not globally representative, especially if there are any systematic problems with individual data constraints, which may be the case for the event-rate data as discussed above and in Appendix C). For those interested in details, the individual normalized slip-rate and event-rate residuals for each segment are listed in the companion file: Test1_A_FaultNormResids.xls (available from the above URL).

Slip-Rate Reduction:

The following three parameters lead to a possible slip-rate reduction on Type-A faults:

"*Fract MoRate to Background*"
"*Fraction Smaller Events & Aftershocks*"
"*Coupling Coefficient*".

All of these are discussed extensively in the main body of this report. "*Fract MoRate to Background*" reflects the fact that our deformation models (i.e., slip rates on Type-A, -B and -C sources given in Appendix A) were defined to accommodate the entire regional deformation, so that some fraction must be removed to avoid double counting with respect to the background

seismicity. The second accounts for the amount of moment on each fault released by events smaller (relative to the lowest magnitude in the segmentation model) and aftershocks. The coupling coefficient represents the fraction of moment between the upper and lower seismogenic depths that is released in earthquakes (as opposed to aseismic moment release, like afterslip, for example). For reasons described in the main body of this report, the total moment-rate reduction for all these parameters combined has been set as 10%. This is applied by the following default settings: "*Fraction Smaller Events & Aftershocks*" = 0.1, "*Fract MoRate to Background*" = 0.0, and "*Coupling Coefficient*" = 1.0. However, the net effect is the same if the 10% is applied in any one of the three parameters (or split between them). This means that the slip rates on all Type-A fault segments are reduced by a factor of 0.9 in Equation Set (1) above.

For comparison, the following file lists results obtained by setting "*Fract MoRate to Background*" = 0.0, "*Fraction Smaller Events & Aftershocks*" = 0.0, and "*Coupling Coefficient*" = 1.0 (zero slip rate reduction):

Test2_A_FaultRupRates.xls

(available from http://www.WGCEP.org/resources/documents/UCERF2_FinalReport).

For moment-balanced models the influence of this slip-rate reduction is, on average, a proportionate reduction in rupture rates.

Mean Mag Correction:

The "*Mean Mag Correction*" parameter enables additional epistemic uncertainty to be applied to the magnitude-area relationships. For example, the NSHMP 2002 model has branches that add +/-0.2 magnitude units to the mean values given by the *Ellsworth-B (WGCEP, 2002, Eq 4.5b)* and *Hanks & Bakun (2002)* Relationships. An earlier version of this model (ERM 2.2) utilized a narrower range of +/-0.1 magnitude units. Results obtained for the +0.1 care are in:

Test3_A_FaultRupRates.xls

(available from http://www.WGCEP.org/resources/documents/UCERF2_FinalReport)

and results for the -0.1 case are in:

Test4_A_FaultRupRates.xls

(available from http://www.WGCEP.org/resources/documents/UCERF2_FinalReport).

For moment-balanced models a "*Mean Mag Correction*" of +0.1 reduces rates by about 30%, on average, and a value of -0.1 increases rupture rates by about 40%. Note that this epistemic uncertainty was eliminated in ERM 2 for reasons discussed in the main text.

Deformation Model:

As discussed in Appendix A, the current WGCEP has defined six different deformation models (D2.1, D2.2, D2.3, D2.4, D2.5, and D2.6). For Type-A faults, rates derived from models D2.1, D2.2, and D2.3 are identical to those derived from D2.4, D2.5, and D2.6, respectively.

The default (used above) is D2.1. Deformation model D2.2 differs from D2.1 in that segment slip rates on the S. San Andreas are lower and those on the San Jacinto are higher (Table 2). Results obtained using D2.2 are available in:

Test5_A_FaultRupRates.xls

(available from http://www.WGCEP.org/resources/documents/UCERF2_FinalReport)

(note that this differs from the all-defaults file above, Test1_A_FaultRupRates.xls, only in the rates on the S. San Andreas and San Jacinto faults. As expected, D2.2 increases rates of events on the San Jacinto and lowers them on the S. San Andreas in the moment-balanced solutions (exact differences are also quantified below in Tables 3 and 5).

Deformation model D2.3 differs from D2.1 in that segment slip rates on the S. San Andreas are higher and those on the San Jacinto are lower. Results obtained using D2.3 are available in:

Test6_A_FaultRupRates.xls

(available from http://www.WGCEP.org/resources/documents/UCERF2_FinalReport).

Relative to D2.1, D2.3 decreases rates of events on the San Jacinto and increases them on the S. San Andreas in the moment-balanced solutions (exact differences are also quantified below in Tables 3 and 5).

Rupture Magnitude Frequency Distributions:

An important implementation detail is that each rupture is given a Gaussian magnitude-frequency distribution with an adjustable sigma and truncation level (the latter defining the last non-zero value on either side of the distribution). We have followed WGCEP-2002 in assigning default values as follows: "*Mag Sigma*"=0.12 and "*Truncation Level*" 2 sigma. We also account for the fact that, with such a range of magnitudes, the average slip is not the same as the slip of the average magnitude (an important distinction with respect to moment balancing). Furthermore, finite discretization of the magnitude-frequency distribution (*e.g.*, where the bins are centered) produces up to ~1.5% changes in some rupture rates.

Final Chosen Solutions

The previous section described the influence of various parameters, and gave access to extensive inversion results that readers can mine to the extent they're interested. The purpose of this section is to zero in on the set of solutions adopted by the present working group, showing how well each model fits the data. A comparison with previous models, including the total implied magnitude frequency distributions for each fault, will be provided later in the Results and Implications section below after presenting the un-segmented model option.

The present working group has adopted three sets of logic-tree branches for the segmentation-based models. The first branch is for the alternative deformation models D2.1, D2.2, and D2.3 as described above. These only influence rates on the Southern San Andreas and San Jacinto Faults. The second set of branches is for the following:

"*Wt On A-Priori Rates*" = 1e10 (called the "A-Priori" model)

"*Wt On A-Priori Rates*" = 1e-4 (called the "Moment Balanced" model)

The former stipulates that the a-priori rates be left unchanged (in spite of how well they fit the slip-rate data), and the latter constitutes the model that is closest to the a-priori rates, but that also fits the slip-rate data exactly (moment balanced). No inversion is really necessary to get the former. However, an important implementation detail for this case is that rates listed as "Unknown" or "Unlikely" in the a-priori model are set to zero (thus, the same final model can be obtained from the inversion by using the "*Wt On A-Priori Rates*" listed above and setting the "*Min Fraction for Unknown Ruptures*" and "*Min Fraction for Unlikely Ruptures*" parameters to zero). For the Moment-Balance branch, the values of "*Min Fraction for Unknown Ruptures*" and "*Min Fraction for Unlikely Ruptures*" are set to the defaults listed in Table 1. Note that the alternative deformation models will have no influence on the A-Priori models (because they ignore slip rates).

The final set of logic-tree branches is for:

"*Mag-Area Relationship*" = *Ellsworth-B (WGCEP, 2002 , Eq 4.5b)*

"*Mag-Area Relationship*" = *Hanks & Bakun (2002)*.

The justification for these two options is given in Appendix D and discussed in the main report. All other parameters remain as the defaults listed in Table 1.

The final magnitudes and rupture rates for the A-Priori versus Moment Balanced and *Ellsworth-B (WGCEP, 2002 , Eq 4.5b)* versus *Hanks & Bakun (2002)* branches are listed in Table 3, and the associated segment rates are listed in Table 4. Tables 5 and 6 give rupture and segment rates, respectively, for the alternative deformation models on the S. San Andrea and San Jacinto Faults. We now discuss how well these models fit the data for each fault

Figure 8 gives the normalized slip-rate and event-rate residuals obtained when the a-priori rates are left unaltered and when applying *Ellsworth-B (WGCEP, 2002 , Eq 4.5b)*. Figure 9 is a similar plot but for *Hanks & Bakun (2002)*. The large normalized slip-rate residuals exemplify the need for moment balancing. The figures described next (Figures 10 to 16) show how well each logic-tree branch fits the data constraints on each fault (results for the alternative deformation models are left out for brevity, but are qualitatively similar).

Elsinore Fault:

Shown in Figure 10 is the predicted versus observed segment slip-rate and event-rate data for the four models on the Elsinore fault (see the caption for important details). The segment event rates implied by the a-priori model generally match the data (as expected since event-rate data are used to construct the a-priori models). The exception is on the Temecula segment (segment #3), where the discrepancy is due to different values being given for different average event-rate estimation techniques (the a-priori models were constructed using the "time/intervals rate" estimates in Table 7 of Appendix C, whereas the comparisons here use the "Poisson rate" estimates of that table). As discussed above, such differences in "best estimate" event rates from paleoseismic data are one of the reasons we have not include this constraint in the inversion. The moment-balanced models obviously improve the fit to segment slip rates (since they are forced

to match), while not violating the event rate data any more than the a-priori models. Note that the moment-balanced models for rupture rate contain nonzero rates for all single and multiple segment combinations; this is due to the minimum rupture rate applied to all segment combinations and results in a more uniform behavior for the fault as a whole than the a-priori model.

Garlock Fault:

As shown in Figure 11, the a-priori and moment balanced models are quite similar in character but the a-priori models fit the event-rate data well, but do not match the slip-rate data on the Central Garlock (GC) segment. Moment balancing fixes the slip rate, but is barely consistent with the event-rate data. The relative rates of different rupture combinations is well matched for both models. Moment balancing is accomplished by increasing the rate of the largest ruptures, which almost doubles the moment while keeping the net event rate within observational bounds.

San Jacinto Fault:

Figure 12 shows results for the San Jacinto fault. The San Jacinto fault is very difficult to model because there is very little event rate information, the slip rates on adjacent sections varies rapidly and the amount of displacement associated with historic (small) and the most recent prehistoric earthquakes (large) varies dramatically from section to section. Unaltered moment-balancing inversions for this fault produce a rate for single Clark-segment events that is considered to be very unlikely. Therefore, we gave a very high weight for the a-priori rate on this segment alone when moment balancing, which effectively constrained it to be exactly the minimum defined for "Unlikely" rupture on this fault. This constraint prevents the "moment balanced" model from matching the slip rates exactly for adjacent sections as well. The a-priori and moment balanced models match the limited event rate data equally well, and both capture the variability in segment rupture rate well, with the moment-balanced model smoothing the variability between segments with zero and nonzero values in the a-priori model. Magnitudes and rates for the alternative deformation models are listed in Table 5 and the associated segment rates are in Table 6.

Southern San Andreas Fault:

Figure 13 shows results for the southern San Andreas fault. The a-priori model tends to over-predict the slip rate for the central part of the fault, especially for the Hanks and Bakun Mag-Area relationship because the recurrence and displacement per event data combine to produce a higher slip rate than the inferred slip rate for this part of the fault. The event rate data are very similar for the a-priori and moment balanced models and are less variable than the actual recurrence data. At the southern end of the fault, the moment balanced model better fits the sharp decline in slip rate and recurrence through segments 8 and 9 but over-predicts the rate for the Coachella segment, which is matched (barely) by the a-priori model. Note that the high event rate at the northern end of the fault (Parkfield) is fixed by historical seismicity.

The rupture rate for individual and multi-segment ruptures is remarkably consistent for the a-priori and moment balanced models. This is because the a-priori model was constructed largely from the correlation of events between paleoseismic sites, which controls the relative frequency of different rupture combinations, and the along strike slip rate, which controls the moment balance, so satisfying both (as the a-priori model does – see Appendix E) generates a

model consistent with both the a-priori and moment balanced models. Magnitudes and rates for the alternative deformation models are listed in Table 5 and the associated segment rates are in Table 6.

Northern San Andreas Fault:

As shown in Figure 14a, the a-priori models tend to over-predict the slip rate. This can be explained by the fact that the a-priori models come from the average WGCEP-2002 rates, which included some finite weight on the Wells and Coppersmith (1994) and Ellsworth-A magnitude-area relationships. Including these latter two relationships implies a lower average magnitude for each rupture, and therefore a lower overall slip rate. In other words, the magnitudes we are assigning to these ruptures are larger than the averages of the WGCEP-2002, so we are over-predicting slip rates since their models were moment balanced (on average).

Moment balancing this model causes the rate of full fault ruptures (i.e., 1906-type events) to go from one every 352 years (in the a-priori model) to one every 1019 years using Ellsworth B and 3268 using Hanks & Bakun. The section event-rate data are still fit well with these moment-balanced models. For comparison, Figure 14b shows results for the case where "*Mag-Area Relationship*" is set as *Ellsworth-A (WGCEP, 2002, Eq 4.5a)* and *Somerville (2006)* (the latter being equivalent to Wells and Coppersmith (1994). As expected, the rate of 1906-type events is higher because there is less average slip per event from these models. Another difference between the WGCEP-2002 model and that adopted here is the value of "*A-Fault Slip Model*". We have adopted the *Tapered Ends* ($[Sin\ (x)]^{0.5}$) option, whereas WGCEP-2002 applied the *WGCEP-2002 Model* ($D_{sr} \propto v_s$). Results for the latter are shown in Figures 14c and 14d for the four magnitude-area relationships.

As can be seen from these comparisons, a fundamental problem is that the preferred Mag-Area relationships for this Working Group are inconsistent with the strongly held view of the 2002 Working Group that full-fault (1906-type) rupture is the dominant mode for the northern San Andreas fault. With the Hanks and Bakun Mag-Area relationship, for example, if all of the moment were put into 1906 ruptures they would occur approximately every 500 years, which is inconsistent with all of the available paleoseismology which tells us that events occur on the northern San Andreas fault about every 200 years (and possibly every one hundred years on the Santa Cruz section).

Hayward-Rodgers Creek Fault:

As shown in Figure 15, the a-priori models over and under-predict the slip rates for the Ellsworth B and Hanks and Bakun magnitude-area relationships, respectively. The a-priori models also over-predict the event rate for the Northern Hayward segment (HN, segment #2). Working Group 2002 suggested that this is because the observed event rate at the associated site is considered a lower estimate due to likely missed event, so the discrepancy is desirable. Moment balancing both improves and worsens the fit to event-rate data (depending on the magnitude-area relationship). Again, this is due to the fact that the a-priori models, generated by Working Group 2002, were tailored to fit a mixture of Mag-Area relationships that included Ellsworth-A and Wells and Coppersmith (1994); individual Mag-Area relationships produce higher or lower results.

The relative rate of single and multi-segment ruptures is very consistent between the a-priori and moment balanced models. Like the southern San Andreas, this is because the a-priori model was essentially constructed by moment balancing the inferred frequency of rupture types.

Calaveras Fault:

As shown in Figure 16, the a-priori model fits the one event-rate constraint pretty well, but under-predicts the slip rate for the Hanks and Bakun (2002) magnitude-area relationship. Similarly, the Hanks and Bakun (2002) magnitude-area relationship cannot quite fit the event rate. Like the Hayward, the relative frequency of rupture rates is similar for both models, due to how the a-priori model was constructed.

Unsegmented Models

As an alternative to the segmentation-base models described above, we have also implemented an unsegmented model option for each Type-A fault. There are only two sets of logic-tree branches here: one for the Ellsworth B vs Hanks and Bakun magnitude-area relationship, and one for the alternative deformation models. We assume the magnitude frequency distribution has a constant rate (b-value = 0) between magnitude 6.5 and an upper magnitude that is computed from total fault area using the given magnitude-area relationship. The rate of events is calculated from the total fault moment rate. Finally, we assume that ruptures for a given magnitude have a uniform probability of occurring anywhere along the fault. Data for these unsegmented models are listed in Table 8 (along with important notes), and magnitude-frequency distributions are presented in the next section. The b-value of 0 was chosen because it is similar to that seen for the segmented models (shown below), and because we obtained significantly higher event-rate residuals applying a b-value of 0.8.

A couple of implementation details are worth noting. First, for the purpose of "floating" ruptures down the faults in hazard calculations, overlapping fault sections on both the Elsinore and San Jacinto fault have been combined into single, non-overlapping sections (with a consequent reduction in the total length, area, and moment rate of the fault). Second, because the San Jacinto fault has a branch (meaning a "y" shape), this fault has been split into two different unsegmented models ("San Bernardino" through "Clark" sections versus "Coyote Creek through "Superstition Mtn" sections), in part because the large step over between the two is thought to impede through going rupture.

A manifestation of assuming uniform location probability for ruptures along the fault is that slip rates taper toward the ends. This can be seen in the average segment slip-rates implied by this un-segmented model plotted at the bottom of Figures 10 to 16. The predicted slip rates fit those observed well for the San Jacinto and Elsinore faults, because observed slip rates taper at the end of these faults, but the match is not so good for the other faults, especially on the San Andreas. We explored the possibility of increasing the rate of small events toward the ends, but this did not fill in the slip-rate deficits (not even by changing the b-value as well). The event-rates predicted by the un-segmented model for each magnitude-area relationship are listed in Table 7 for the sites where we have paleoseismic observations (see caption for important details). The predictions at about 20 percent of the sites fall outside the 95-percent confidence bounds for the observations. Some are too high and some are too low, so attempts to modify the assumed b-value to improve the fit would have to be made on a fault-by-fault basis.

It should be noted that the WGCEP-2002 included an unsegmented model option in terms of their "floating' earthquake model. However, they assigned a single magnitude for these floating earthquakes (with aleatory uncertainty represented as a Gaussian distribution with a standard deviation of 0.12 and truncated at +/- two sigma), whereas we have applied a broader range of magnitudes and have assigned a uniform distribution (b-value = 0). Our justification is that we feel a broader range of possibilities should be accommodated.

Results and Implications

Figure 17 gives a logic-tree representation of the final models chosen for the type-A faults. There are three branches for alternative deformation models, two branches for the Ellsworth-B versus Hanks and Bakun magnitude-area relationship, and three branches for un-segmented, moment balanced, and a-priori models. Thus, there are a total of 18 branches, although the alternative deformation models only influence the S. San Andreas and San Jacinto faults. The weights for the alternative deformation models are developed in Appendix A, and the choices and weights for the magnitude-area relationships are given in Appendix D (and are the same as those applied in the NSHMP (2002) model). The a-priori and moment-balanced options for the segmented models are given equal weight because neither, when averaged over all faults, provides a superior fit to the overall data. Finally, we give 10-percent weight to the un-segmented versus segmented model, which is roughly consistent with the average value adopted by WGCEP (2003). Figure 18 shows the magnitude-frequency distributions for each rupture model on each fault, along with the total (weight average) implied by the logic-tree-branch weights.

Although the branch on the segmented versus un-segmented model in Figure 17 implies an epistemic uncertainty, it can alternatively be thought of as aleatory (the question being whether it behaves one way or another, or exhibits both behaviors over the long term). The WGCEP (2003) treated their floating earthquakes as an aleatory combination with the segmented model. Most currently working group members do not believe that either the segmented or un-segmented models are a strictly correct representation of the true behavior. What we believe, however, is that the combination defined here represents the currently best available for modeling hazard. Furthermore, whether this aleatory or epistemic has no influence on the mean hazard and loss estimates, which is of primary interest for now.

The final branch weights were established at a series of meetings among the authors of this document. Specifically, all figure presented here, as well as others not shown, were carefully scrutinized on a fault-by-fault basis. Considerable thought was given to varying branch weights among the different faults (based on the degree to which each model fit the data), but in the end we were reluctant to apply such customization give inherent limitations of each type of model.

Comparison with WGCEP UCERF 1

Our basis for comparison with respect to previous studies is the time-independent option of UCERF 1 (Petersen et al., 2007). Where available, corresponding UCERF 1 rupture rates and magnitudes have been listed in Table 3, and the total magnitude-frequency distributions have been plotted in Figure 18 (with bold black lines, which can be compared to our total, weight-averaged results shown with bold red lines).

For the N. SAF, Hayward-Rodgers Creek, and Calaveras faults, UCERF 1 results come from WGCEP-2002. However, the rates listed in Table 3, which come from the NSHMP-2002 implementation of the WGCEP-2002 model (which UCERF 1 is based on), are generally ~6% higher than those listed in Table 4.8 of the WGCEP-2002 report. The reason for this difference is that NSHMP-2002 did not want any moment removed for smaller earthquake (the "Gutenberg-Richter tail" applied by WGCEP-2002), and so their rates are higher. Note that the WGCEP-2002 model also included floating earthquakes, which are not listed in Table 3 but are included in the magnitude-frequency distribution plots of Figure 18. The fact that the agreement in Figure 18 between the old and new is quite good is not surprising given our a-priori models for these

faults are based on the WGCEP-2002 results (see Appendix K for a description of how the a-priori models were developed).

The UCERF 1 results for the Elsinore and San Jacinto Faults are identical to the NSHMP-2002 implementation. The biggest difference for both faults is the inclusion of multi-segment ruptures in the new models (which were not included in the NSHMP-2002 model). This effectively puts more moment into larger events, and consequently lowers the total rate of events by about a factor of ~2.4.

A rupture-by-rupture comparison is not possible for the S. SAF fault because the new model has many more, and generally different, segments defined (thus, no UCERF 1 values are listed in Table 3 for this fault). However, Figure 18 includes a comparison of the magnitude frequency distributions, which agree surprisingly well given the radical difference between models (see Appendix E for a description of the development of the *Geologic Insight* a-priori model)

The Garlock fault was not previously considered a Type-A source, so there are no UCERF 1 results listed in Table 3 or plotted in Figure 18.

Future Improvements

A variety of improvements could be made to the model. For the current version (ERM 2) we have adopted only 18 different models for each fault. While this should be adequate for the needs of both the NSHMP and CEA (because they are interested in only *average* hazard and loss estimates, respectively), other logic-tree branches can and should be implemented at some point if uncertainty analyses are desirable. One potentially important logic-tree branch would include the *Minimum Rate* and *Maximum Rate* a-priori models. However, as discussed above, issues exist with respect to weighting these models in the moment-balancing inversion, so some work on this will be required.

The inversion methodology provides a great deal of flexibility in terms of fine-tuning a solution, whereas we have adopted two relatively simple end members (Geologic Insight a-priori rates left unchanged, and the nearest Moment Balanced solution). Furthermore, we are presently using the segment event-rate data only as a reality check of the models. Certainly further improvements could be made in terms of defining a best model for each fault using the existing inversion methodology. However, this would require fine-tuning on a fault-by-fault basis, which would take more time to document and justify. Furthermore, many working group members are uncomfortable with the segmentation assumption in general, so fine-tuning a model that could be fundamentally flawed is perceived as a potential waste of time (and we'd prefer to spend our time developing a potentially improved overall approach).

We believe the inclusion of the unsegmented model is an improvement. However, further work is needed to make these models match along-fault variations in slip rate (the challenge has more to do with implementing such variations in hazard calculations than defining the model). We also need to try to improve the fit to event-rate data at paleoseismic sites along the fault. Perhaps adjustments of the b-value (currently zero) could be made to improve the fit to these observations, although this would need to be done on a case-by-case basis.

References

Frankel, A., C. Mueller, T. Barnhard, D. Perkins, E. Leyendecker, N. Dickman, S. Hanson, and M. Hopper (1996). National seismic-hazard maps: documentation June 1996, *U.S. Geol. Surv. Open-file Rept. 96-532*.

Frankel, A.D., M.D. Petersen, C.S. Mueller, K.M. Haller, R.L. Wheeler, E.V. Leyendecker, R.L. Wesson, S.C. Harmsen, C.H. Cramer, D.M. Perkins, K.S. Rukstales (2002). Documentation for the 2002 update of the national seismic hazard map, *U.S. Geol. Surv. Open-file Report 02-420*.

Gardner, J. K. and L. Knopoff (1974). Is the sequence of earthquakes in southern California, with aftershocks removed, Poissonian? *Bull. Seis. Soc. Am.* **64**, 1363–1367.

Hanks, T.C, and H. Kanamori (1979). A moment magnitude scale, *J. Geophys. Res.* **84**, 2348-2350.

Lawson, C.L. and D.J. Hanson (1974). Solving Least Squares Problems. *Prentice-Hall*, Englewood Cliffs, New Jersey.

Menke (1989). Geophysical Data Analysis: Discrete Inverse Theory, *Academic Press, Inc.*.

Petersen, M.D., T. Cao, K.W. Campbell, and A.D. Frankel (2007). Time independent and time-dependent seismic hazard assessment for the state of California: Uniform California Earthquake Rupture Forecast model 1.0, *Seism. Res. Lett.* **78**, 99-109.

Working Group on California Earthquake Probabilities (1995). Seismic hazards in southern California: probable earthquakes, 1994-2024: *Bull. Seism. Soc. Am.* **85**, 379-439.

Working Group on California Earthquake Probabilities (2003). Earthquake Probabilities in the San Francisco Bay Region: 2002–2031, *USGS Open-File Report* **03-214**.

Youngs et al. (2003). A Methodology for Probabilistic Fault Displacement Hazard Analysis (PFDHA), *Earthquake Spectra* **19**, 191-219

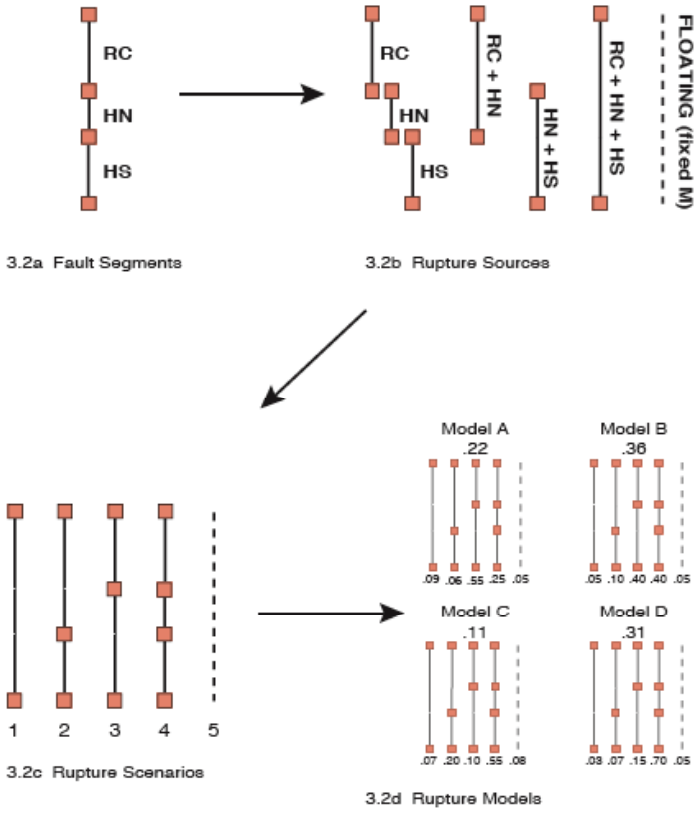

Figure 1. Fault segments, ruptures, scenarios, and models as defined by the WGCEP-2002 (WGCEP, 2003) on the Hayward-Rodgers Creek fault (taken from their Figure 3.2).

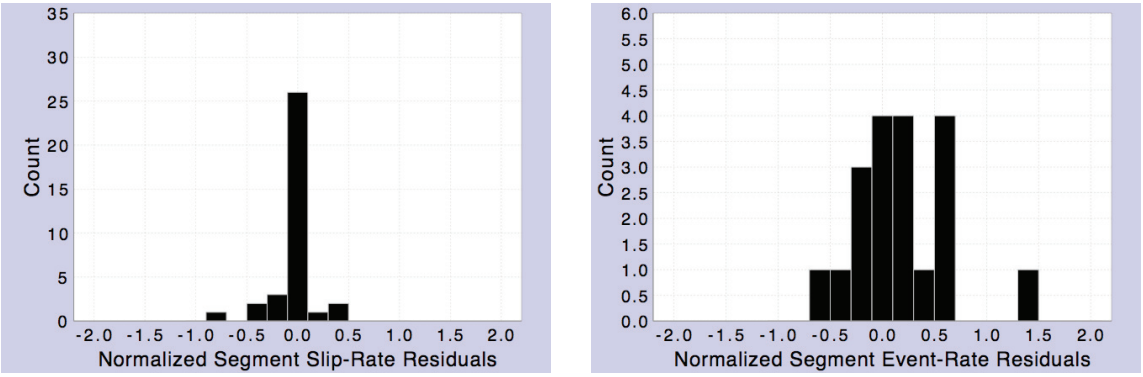

Figure 2. Histogram of normalized residuals for slip rate ($[v_s^{obs} - v_s^{pre}]/\sigma_{v_s}$) and event rate ($[\lambda_s^{obs} - \lambda_s^{pre}]/\sigma_{\lambda_s}$) for all segments and all faults, obtained using default parameter settings (bold typeface values listed in Table 1), except where: "*Relative Wt On Segment Rates*" = 1.0 (to include segment rates in the inversion); "*Min Fraction for Unknown Ruptures*" = 0.0; and "*Min Fraction for Unlikely Ruptures*" = 0.0.

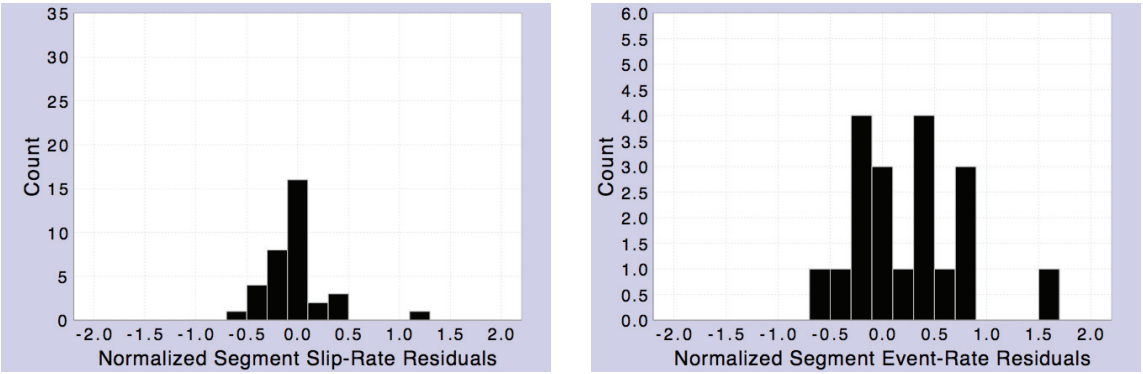

Figure 3. Same as Figure 2, except that "*Weighted Inversion?*" = *false*.

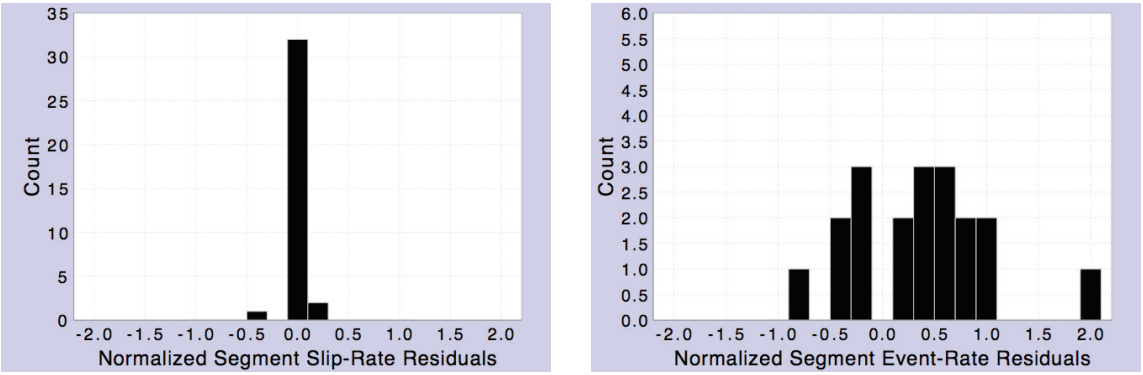

Figure 4. Same as Figure 2, except that "*Relative Wt On Segment Rates*" = 0.0.

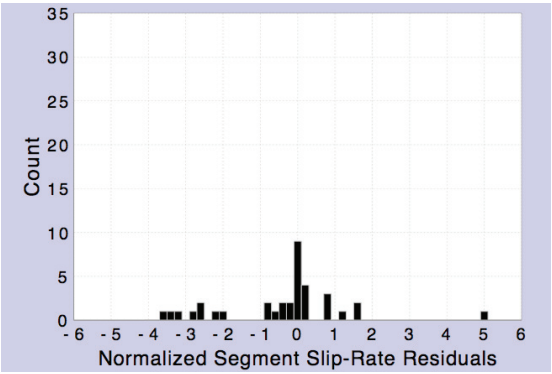

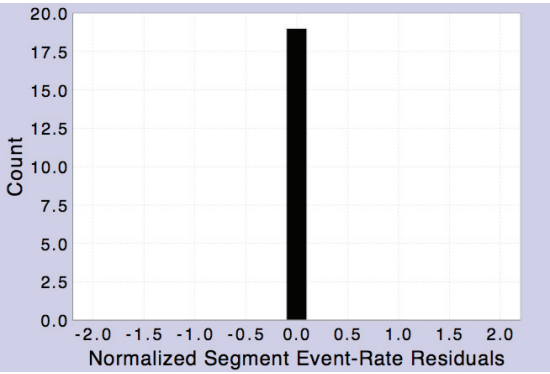

Figure 5. Same as Figure 2, except that "*Relative Wt On Segment Rates*" = 1e7. Note that the scaling is different than in Figures 2-4.

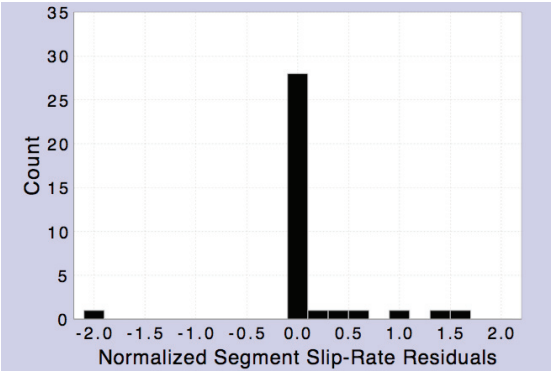

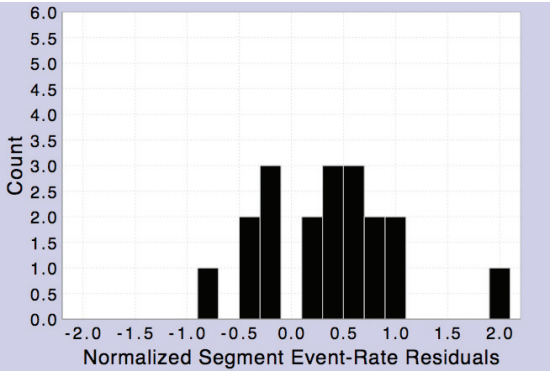

Figure 6. Results for when all parameters have been set to the default values listed in Table 1 (same as Figure 4, but where "*Min Fraction for Unknown Ruptures*" = 0.5; and "*Min Fraction for Unlikely Ruptures*" = 0.1).

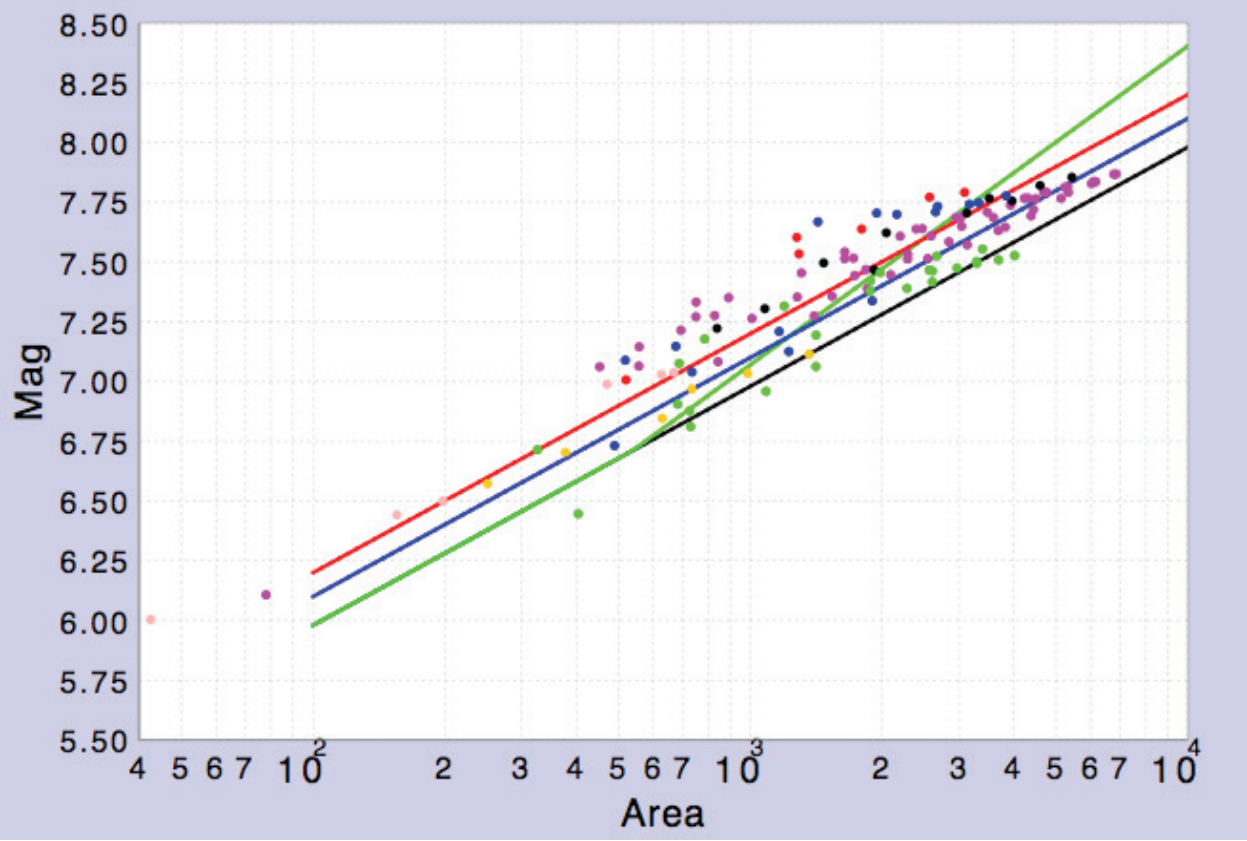

Figure 7. Circles show the magnitudes and areas implied by the *Characteristic Slip* model, color coded for each fault as follows: Elsinore, Garlock, San Jacinto, N. San Andreas, S. San Andreas, Hayward-Rogers Creek, Calaveras. Note that in computing the magnitudes from equations (5) & (6), segment slip rates have been reduced according to the default values for the "*Fract MoRate to Background*", "*Fraction Smaller Events & Aftershocks*", and "*Coupling Coefficient*" parameters (points are simply shifted up or down by the same amount for other values). Also, the segment event rates (λ_s) in equation (5) are computed from the default a-priori rupture rates since data are not available for many fault sections. The lines are the predictions from magnitude-area relationships, color coded as follows: *Ellsworth A (WGCEP, 2002, Eq. 4.5a)* in blue, where Mag=4.1+log(Area); Ellsworth-B (WGCEP, 2002, Eq. 4.5b) in red, where Mag=4.2+log(Area); Hanks and Bakun (2002) in green, where Mag=3.98+log(Area) if Area<537 sq-km, and Mag=3.07+1.333log(Area) otherwise; and Somerville (2006) in black, where Mag=3.98+log(Area).

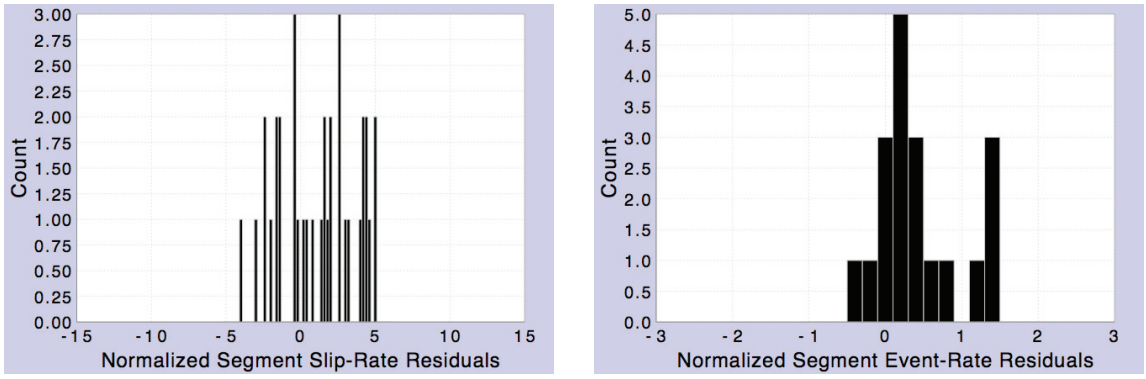

Figure 8. Normalized segment slip-rate and event-rate residuals for all A-faults when the a-priori rates are left unchanged (defaults in Table 1, except "*Wt On A-Priori Rates*" = 1e10; "*Min Fraction for Unknown Ruptures*" = 0.0; and "*Min Fraction for Unlikely Ruptures*" = 0.0). Note that the scaling is different than in Figures 2-4.

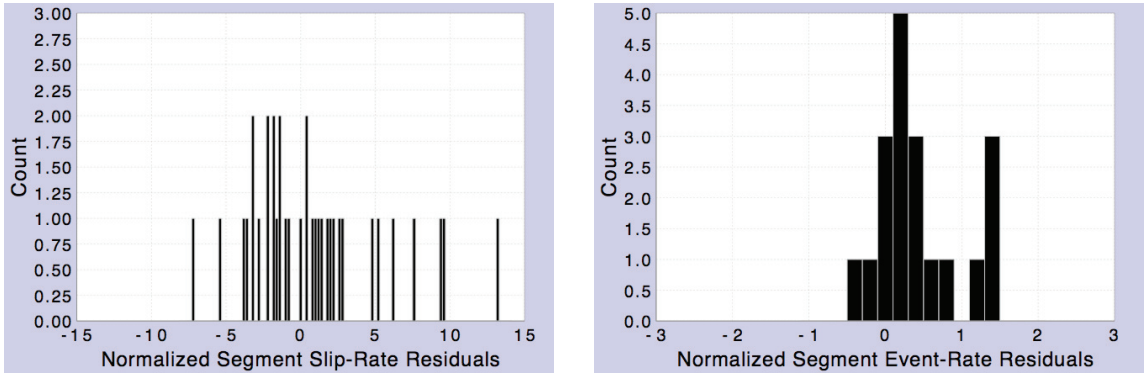

Figure 9. Same as Figure 8, except where "*Mag-Area Relationship*" = *Hanks & Bakun (2002)*. Note that the scaling is different than in Figures 2-4.

Figure 10. The top row of this figure shows how the four segmented models for the Elsinore fault fit the slip-rate data, where the latter come from Table 2 and are shown as red crosses with 95% confidence bounds. The a-priori models are plotted as green lines, and those for the moment-balanced model are plotted as **black lines** (note that moment-balanced models match the slip-rate data exactly, as expected). The left side shows results for the Ellsworth-B magnitude-area relationship, and those for Hanks and Bakun are on the right. The second row is an equivalent comparison for segment event rates, where the data come from Table 8 of Appendix C (reproduced in Table 7 here) and only the 95% bounds are shown given the uncertainties associated with defining a "best estimate". The segment indices are as follows: 1=W, 2=GI, 3=T, 4=J, and 5=CM (where the acronyms are defined in Table 2). The third row plots the rate of each rupture for the a-priori model and the **moment-balanced models** (the rupture indices are defined in terms of segments involved in Table 3). The bottom row shows a comparison of observed segment slip rates (same as in the top row) with the slip rates implied by the **un-segmented model** described in the text.

Figure 10. Caption on previous page.

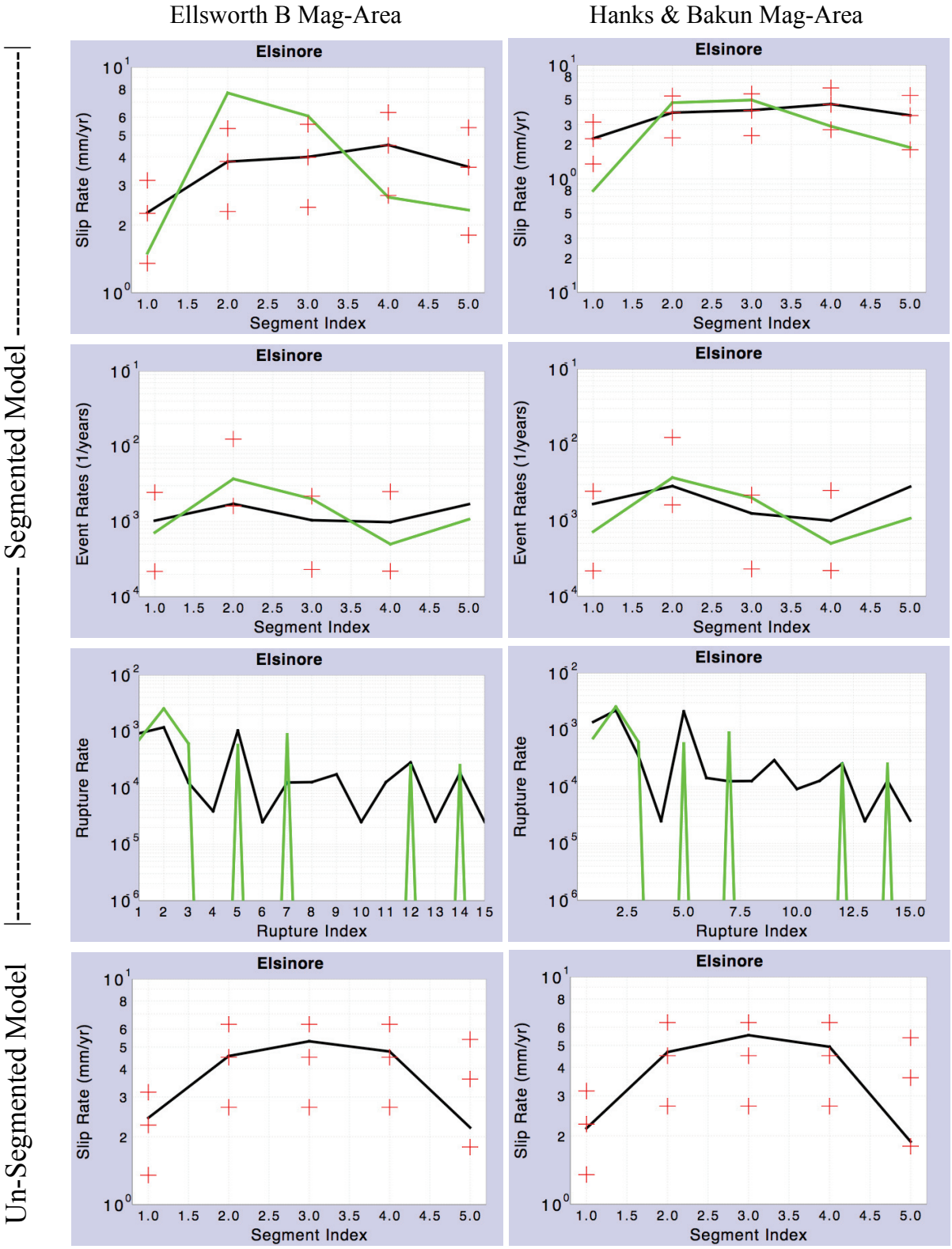

Figure 11. Same as Figure 10, but for the Garlock fault. The segment indices are as follows: 1=GE, 2=GC, 3=GW (where the acronyms are defined in Table 2). Event rate data are only shown where available.

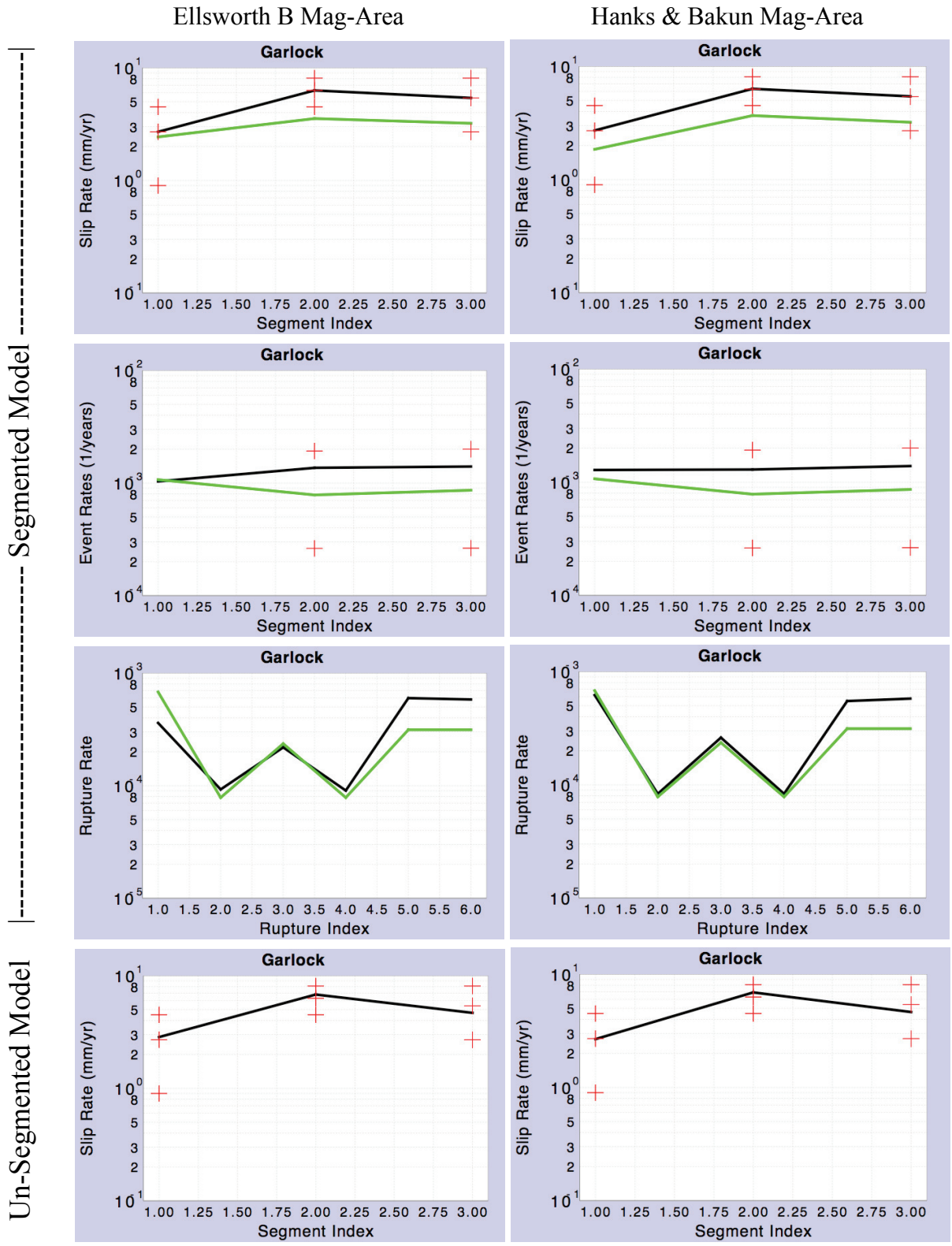

Figure 12. Same as Figure 10, but for the San Jacinto fault. The segment indices are as follows: 1=SBV, 2=SJV, 3=A, 4=C, 5=CC, 6=B, 7=SM (where the acronyms are defined in Table 2). Event rate data are only shown where available. Note that the lower slip-rate confidence bounds for the CC and B segments are not visible because they plot below the lower y-axis limit.

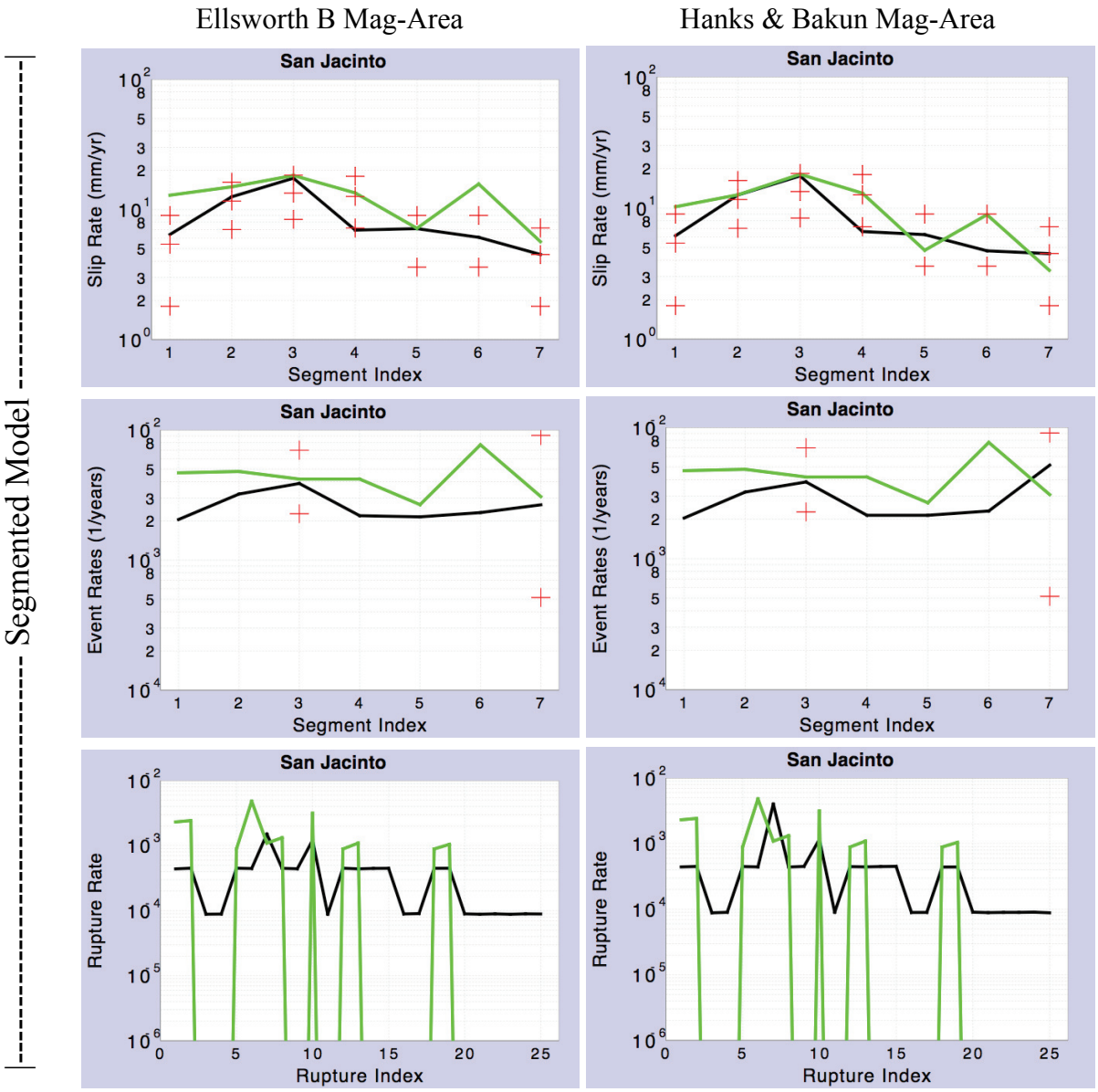

Figure continued on next page

Ellsworth B Mag-Area

Hanks & Bakun Mag-Area

Un-Segmented Model

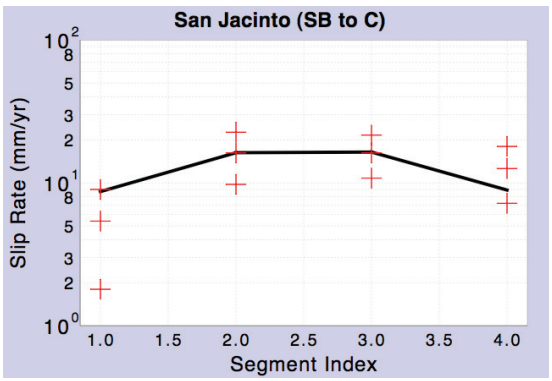

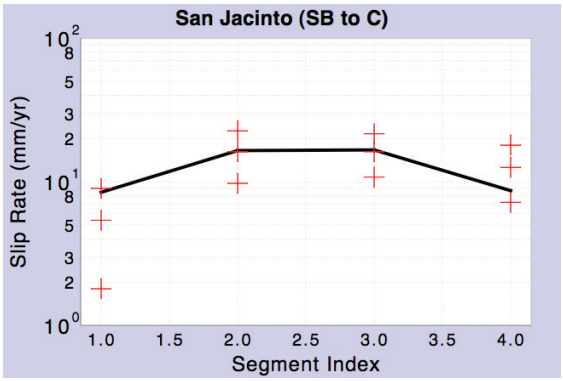

Un-Segmented Model

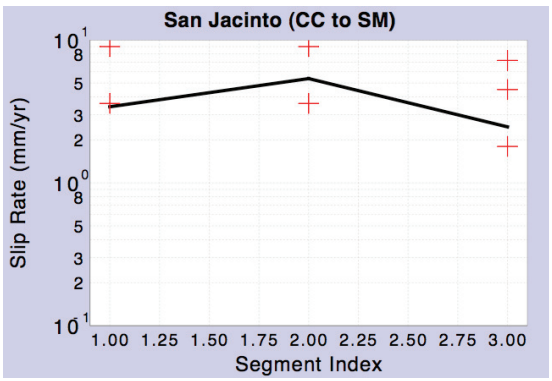

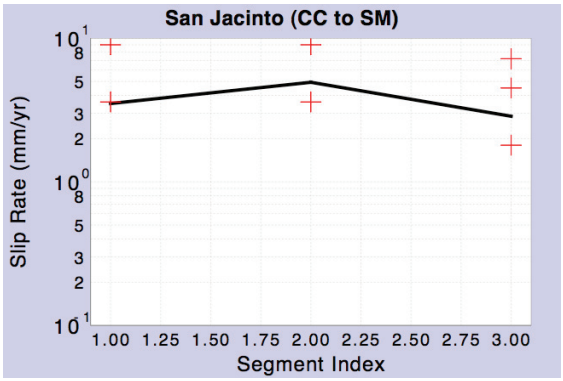

Figure 13. Same as Figure 10, but for the Southern San Andreas fault. The segment indices are as follows: 1=PK, 2=CH, 3=CC, 4=BB, 5=NM, 6=SM, 7=NSB, 8=SSB, 9=BG, 10=CO (where the acronyms are defined in Table 2). Note that segments 6 and 8 have multiple event-rate estimates, which are plotted as slightly offset crosses.

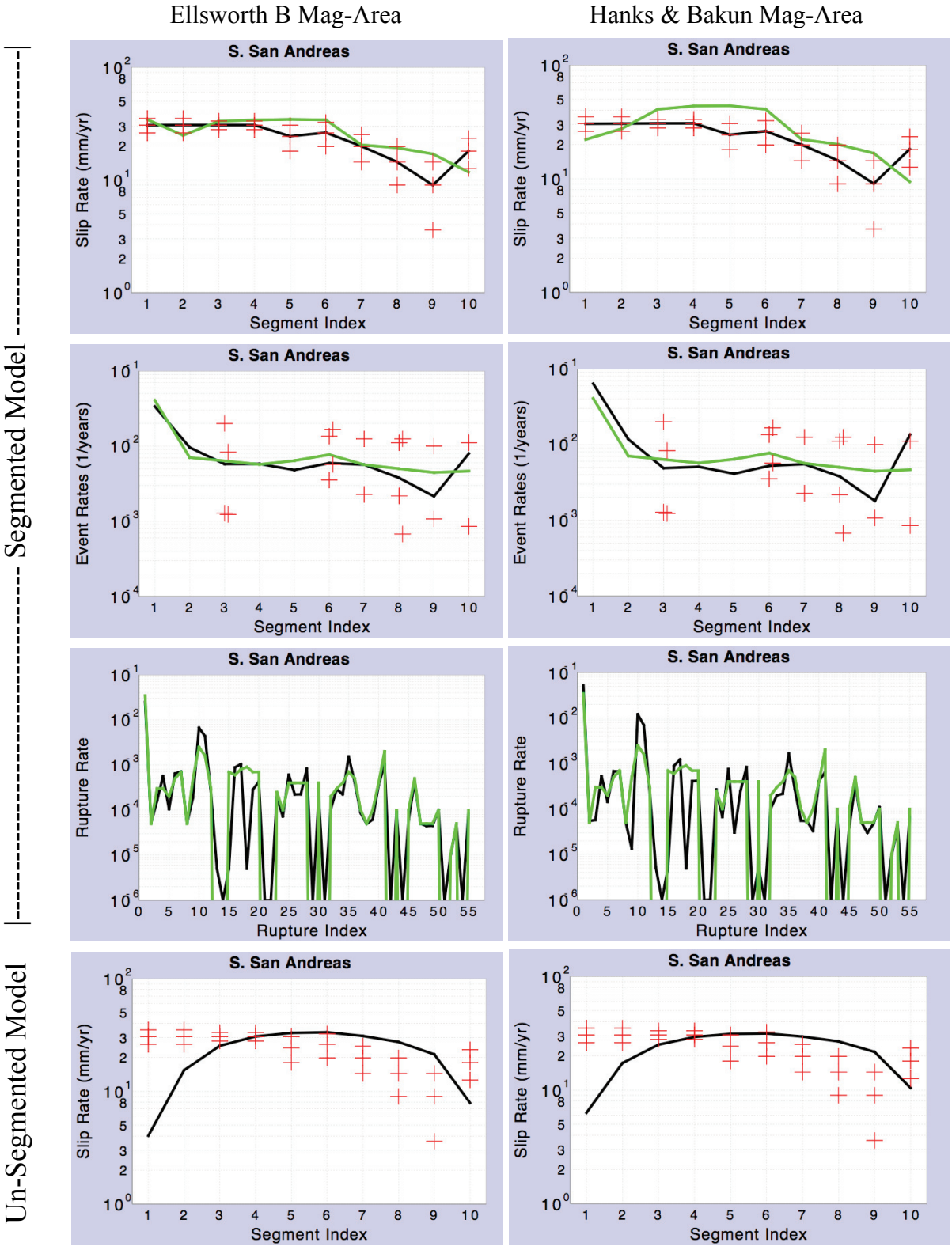

Figure 14a. Same as Figure 10, but for the Northern San Andreas fault. The segment indices are as follows: 1=SAO, 2=SAN, 3=SAP, 4=SAS (where the acronyms are defined in Table 2).

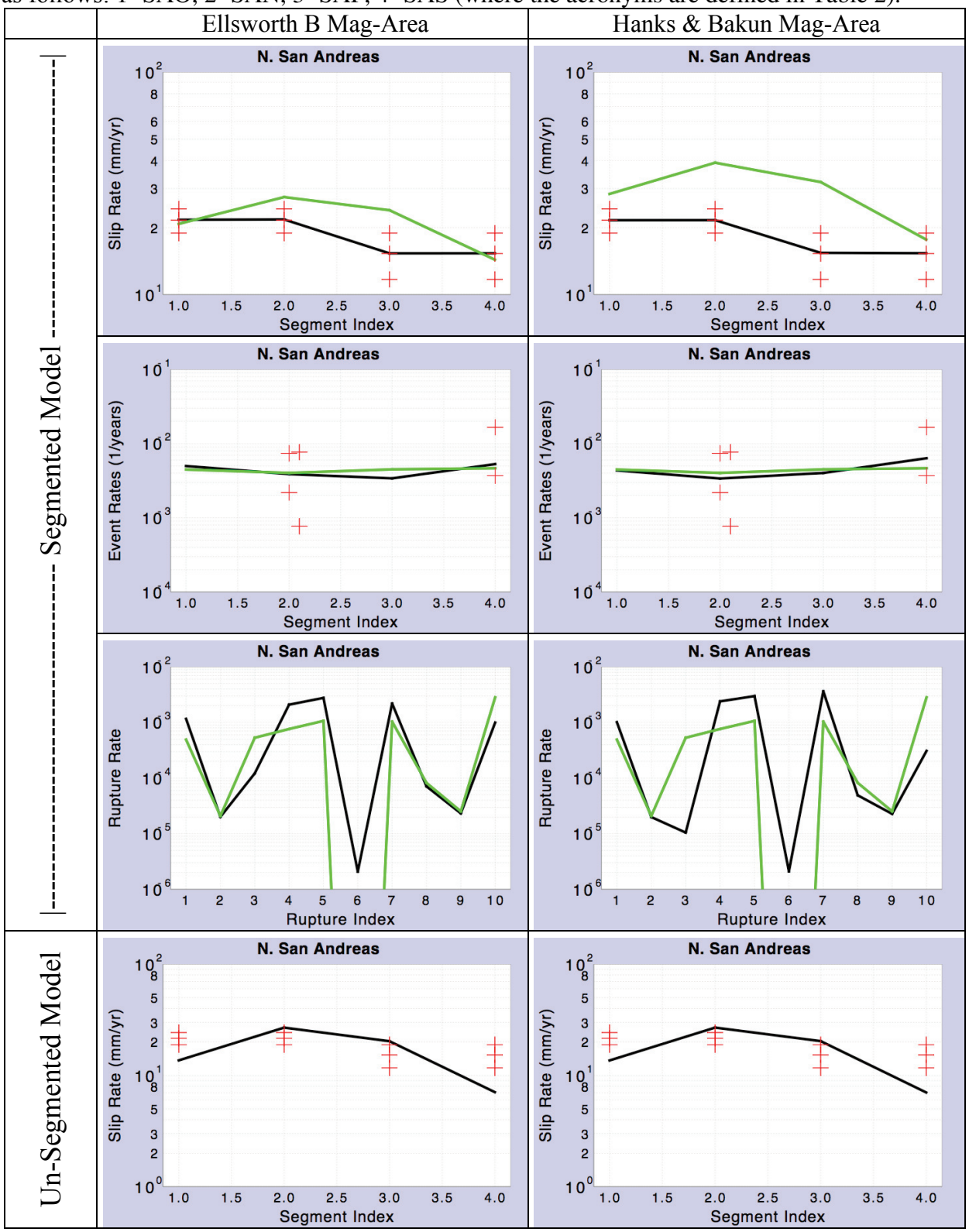

Figure 14b. Same as Figure 14a, except the Ellsworth A and Somerville Mag-Area relationships have been used.

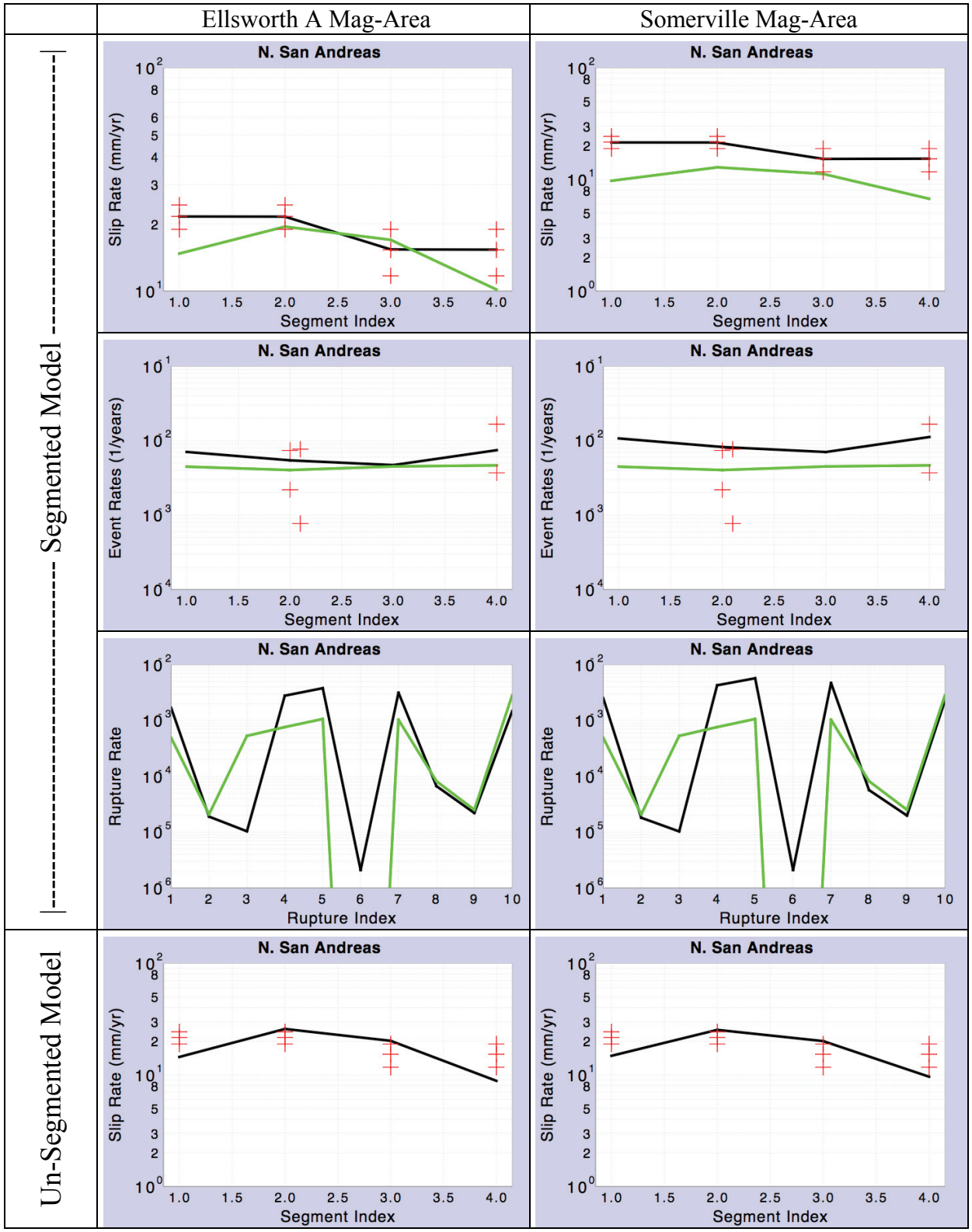

Figure 14c. Same as Figure 14a, except that "*A-Fault Slip Model*" = *WGCEP-2002 Model* ($D_{sr} \propto v_s$). No un-segmented model results are shown because they are the same as in Figure 14a.

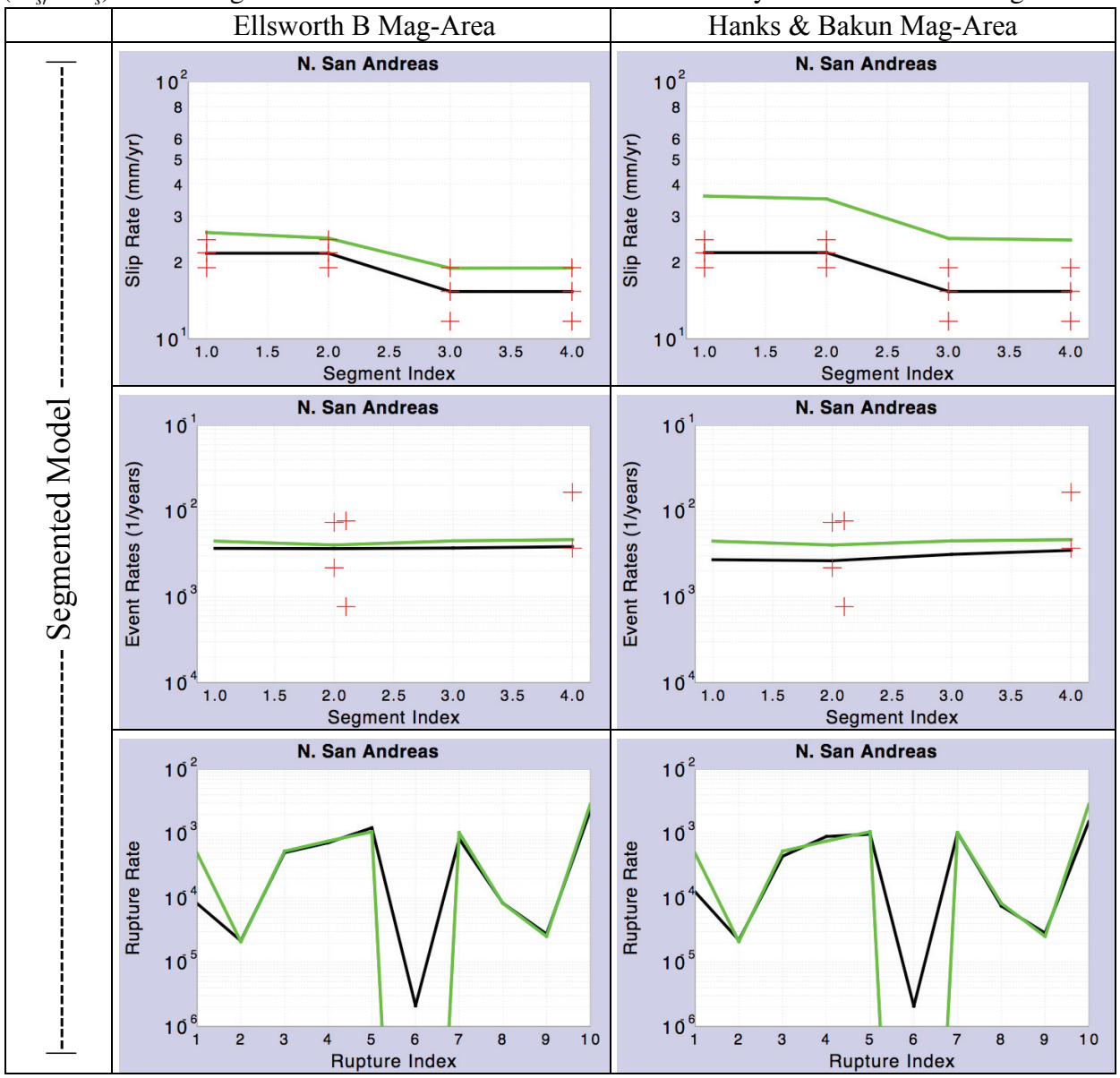

Figure 14d. Same as Figure 14b, except that "*A-Fault Slip Model*" = *WGCEP-2002 Model* ($D_{sr} \propto v_s$). No un-segmented model results are shown because they are the same as in Figure 14b.

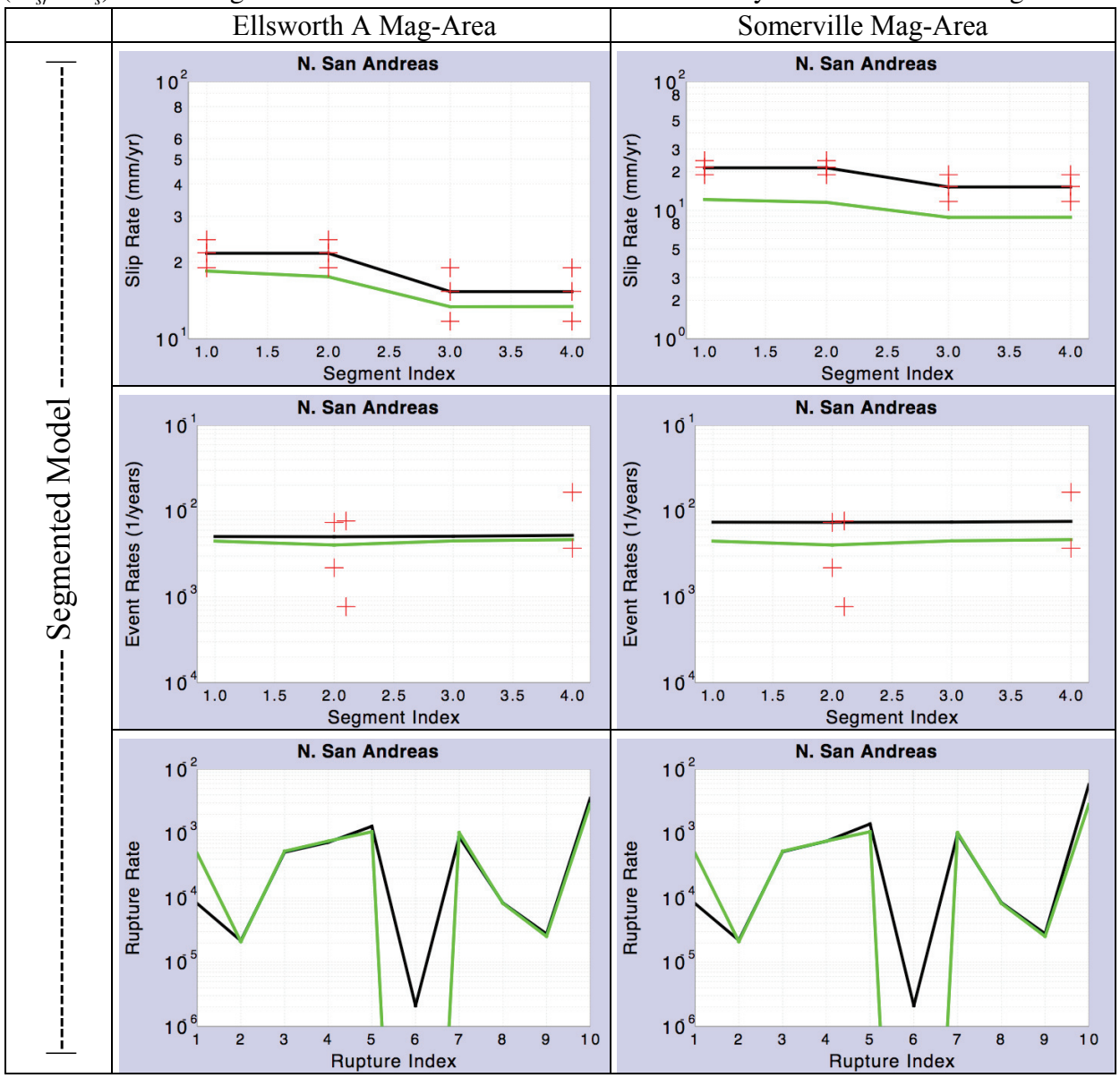

Figure 15. Same as Figure 10, but for the Hayward-Rodgers Creek fault. The segment indices are as follows: 1=RC, 2=HN, 3=HS (where the acronyms are defined in Table 2).

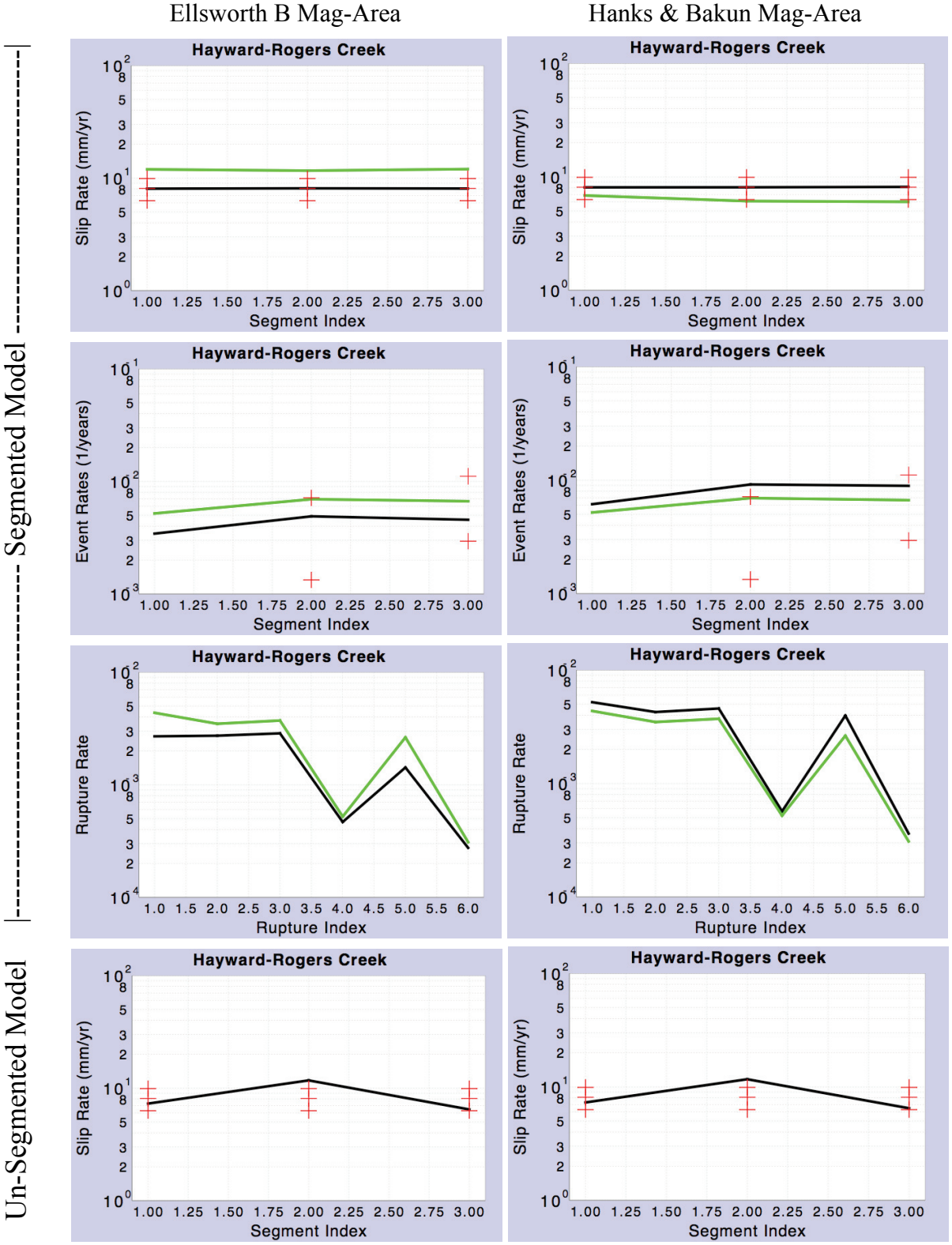

Figure 16. Same as Figure 10, but for the Calaveras fault. The segment indices are as follows: 1=CN, 2=CC, 3=CS (where the acronyms are defined in Table 2).

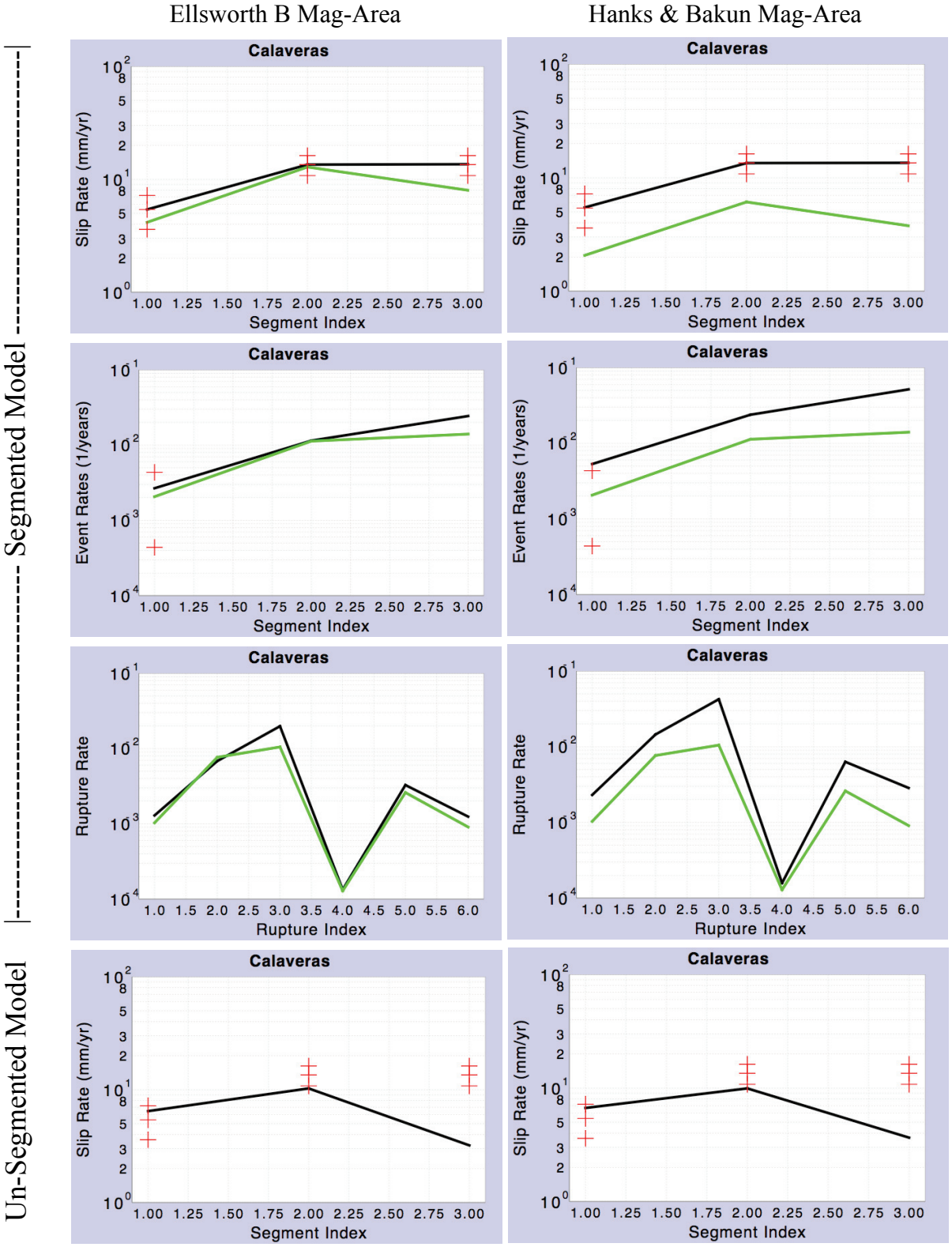

Figure 17. Logic tree for final, chosen A-fault models.

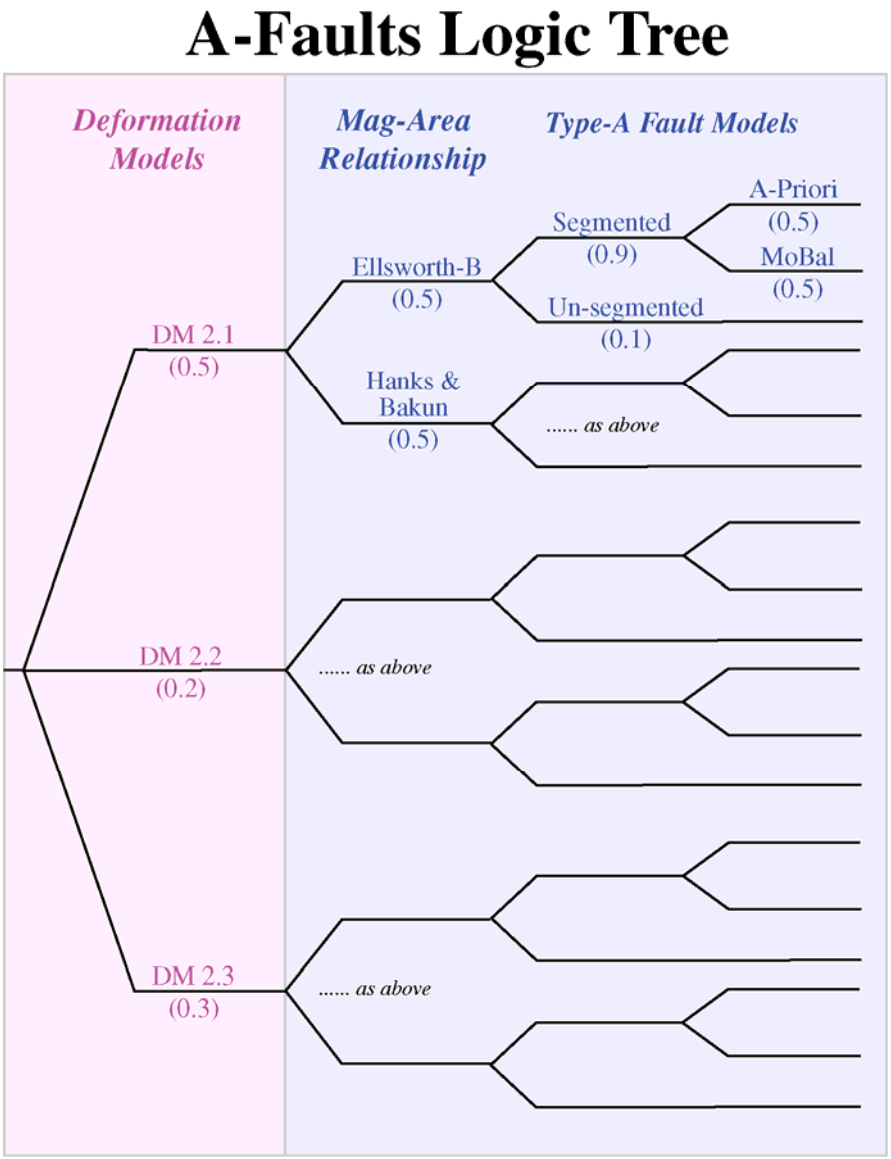

Figure 18. Magnitude frequency distributions (incremental on the left and cumulative on the right) for the seven Type A faults. The plots for individual models are color coded as follows: blue for Moment Balanced with Ellsworth-B Mag-Area Relationship; gray for Moment Balanced with Hanks and Bakun Mag-Area Relationship; Green for A Priori with Ellsworth-B; hot pink for A Priori with Bakun; salmon for unsegmented with Ellsworth-B; yellow for unsegmented with Hanks and Bakun. The **bold red line** is the total for each model (weight averaged according to logic-tree branch weights), and the **bold black line** is the distribution from WGCEP UCERF 1 (equivalent to the WGCEP-2002 Poisson model for the N. SAF, Hayward-Rodgers Creek, and Calaveras, and equivalent to the NSHMP-2002 model for the other faults, except that the S. SAF had an additional model added in UCERF 1 relative to NSHMP-2002. The unsegmented model plots for the San Jacinto fault are the sum of the two sources (the fault was separated into two as described in the text).

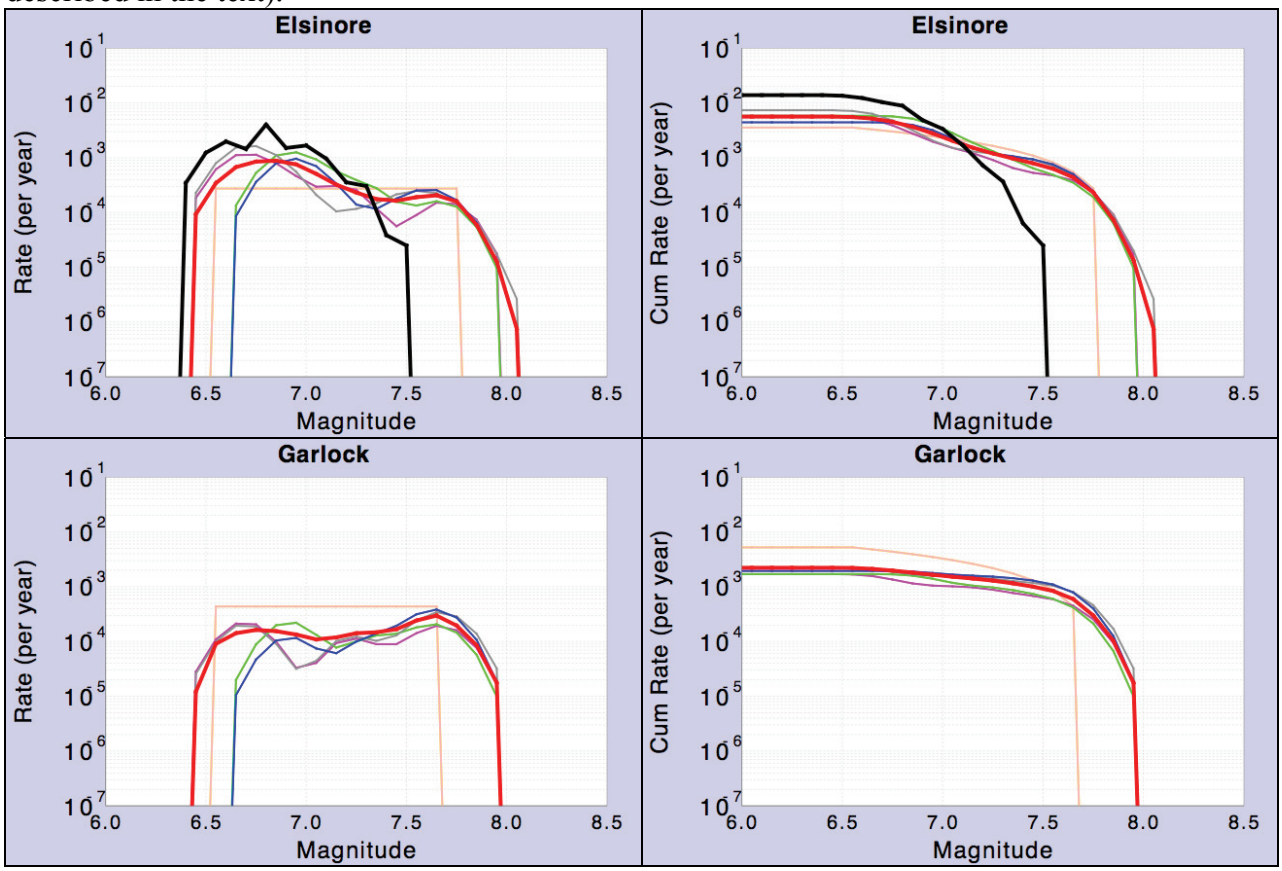

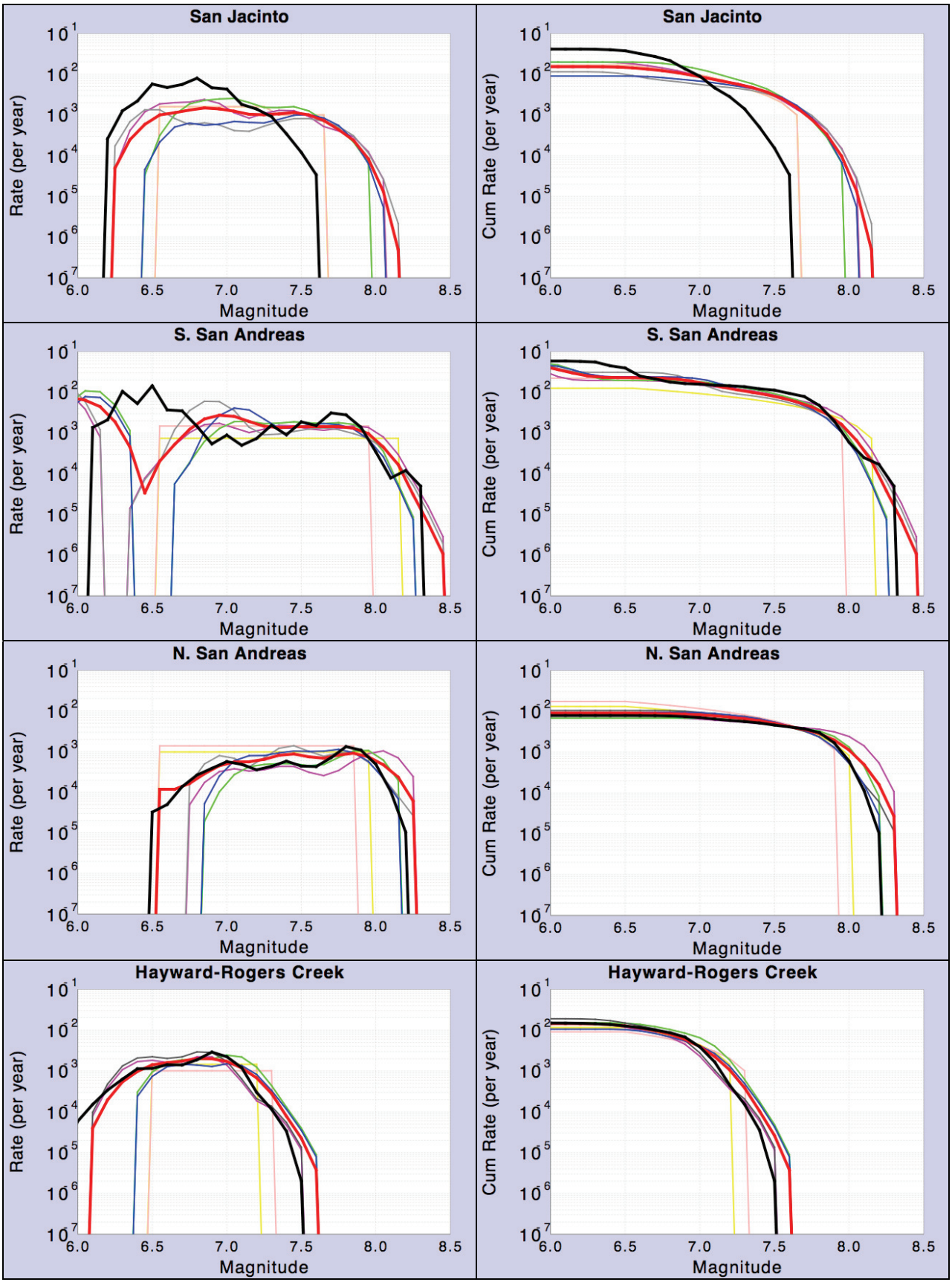
San Jacinto
Rate (per year)
Magnitude
San Jacinto
Cum Rate (per year)
Magnitude
S. San Andreas
Rate (per year)
Magnitude
S. San Andreas
Cum Rate (per year)
Magnitude
N. San Andreas
Rate (per year)
Magnitude
N. San Andreas
Cum Rate (per year)
Magnitude
Hayward-Rogers Creek
Rate (per year)
Magnitude
Hayward-Rogers Creek
Cum Rate (per year)
Magnitude

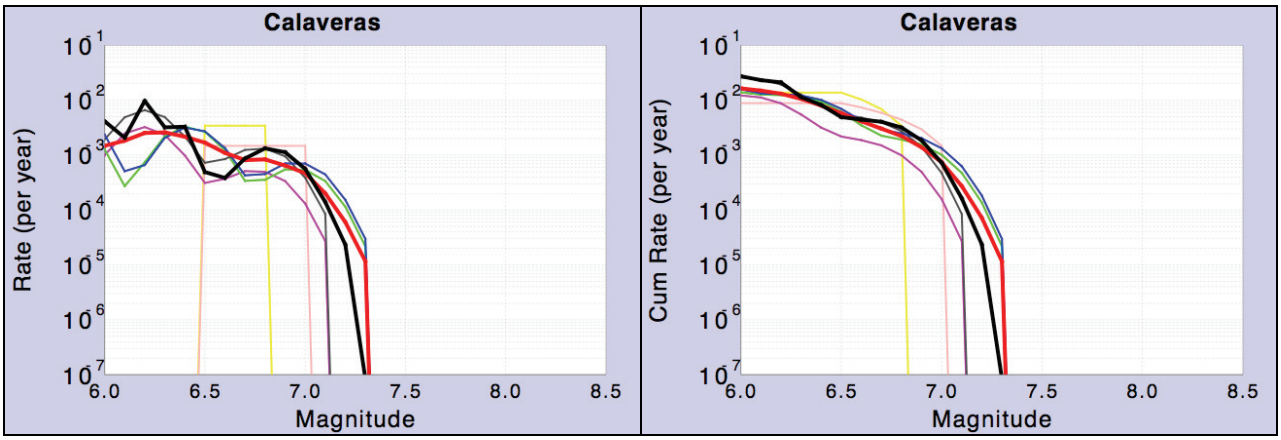
Calaveras
Rate (per year)
Magnitude
Calaveras
Cum Rate (per year)
Magnitude

Table 1. Adjustable parameters (logic tree branches) that Type-A faults depend on. Values listed in bold typeface are the default/preferred values. Numbers in parentheses under "Allowed Values" indicate the applicable range for continuous variables.

Parameter Name	Allowed Values	WGCEP wts	Details
Deformation Model	**D2.1** D2.2 D2.3	0.5 0.2 0.3	These models differ only in a slip-rate tradeoff between the S. San Andreas and San Jacinto Faults. They are approximately equal in model D2.1, relatively higher on the San Jacinto in model D2.2, and lower on the San Jacinto in model D2.3 (see Table 2).
Frac MoRate to Background	**0.0** 0.1 (0.0 to 1.0)	1.0 0.0	The fraction of moment rate in the deformation model accommodated by seismicity not on Type A, B, & C sources (values •1 avoid double counting with respect to background seismicity).
Fraction Smaller Events & Aftershocks	0.0 **0.1** (0 to 1)	0 1	The fraction of moment on faults that is released via smaller earthquakes and foreshocks/aftershocks (for the Gardner Knopoff (1974) definition of the latter).
Coupling Coefficient	**1.00** 0.85 (0-1; 1.0=fully seismic)	1.0 0.0	Fraction of moment released via seismogenic processes (*e.g.*, not afterslip) between upper and lower seismogenic depths. Applies as a reduction of slip rate.
A-Fault Solution Type	Min Rate, Max Rate, **Geol Insight,** Un-segmented	See separate table.	The type of model solution to apply to the A-Fault Sources. Unsegmented models use a GR distribution with a b-value of 0.0.
A-Fault Slip Model	Characteristic Uniform/Boxcar WGCEP-2002 (slip ~ slip rate) **Tapered Ends ($[\sin(x)]^{0.5}$)**	0 0 0 1	Type of slip model to apply to the segmented A-Fault models. Taper based on Biasi & Weldon (2006) and Biasi & Weldon (submitted).
Wt On A-Priori Rates	**1e-4** 1e10 (0 to Inf)	0.5 0.5	This specifies the weight given to a-priori rates in the inversion (Equation-Set (3)), interpreted as the ratio of the rate divided by its uncertainty. A value of 1e-4 leads to a purely moment-balance model, and a value of 1e10 maintains a-prior rates exactly.
Relative Relative Wt On Segment Rates	**0.0** (0 to Inf)	1	The relative weighting of segment rates versus slip rates in the inversion. Setting this to zero means the slip-rate equations are not included.
Weighted Inversion	***Yes*** *No*	1 0	Slip rate and segment rate uncertainty used in the inversion (weighted least squares).
Min Fraction for Unknown Ruptures	**0.5** (0 to 1)	1	Any A-fault rupture flagged with an "Unknown" rate in the a-priori model will be constrained to have a post-inversion rate that is greater than or equal to this number times the minimum rate of all ruptures in the a-priori model.
Min Fraction for Unlikely Ruptures	**0.1** (0 to 1)	1	Same as above, but for ruptures flagged as "Unlikely".
Mag-Area Relationship	Ellsworth-A (WGCEP, 2002 , Eq 4.5a), **Ellsworth-B** (WGCEP, 2002 , Eq 4.5b), Hanks & Bakun (2002), Somerville (2006)	0 0.5 0.5 0	Used for B-fault sources and on A Faults if Characteristic slip model not chosen.
Mag Sigma	**0.12** (0.0 to 1.0)	1.0	Standard deviation applied to Gaussian dist. of characteristic magnitude-frequency distributions (for A- and B-Faults).
Truncation Level	**2.0** (0.0 to 6.0)	1.0	Truncation level (number of sigmas) applied to Gaussian distribution of characteristic earthquakes.
Mean Mag Correction	**0.0** (-0.5 to 0.5)	1.0	Increment added to mean mags computed from a magnitude-area relationship as additional epistemic uncertainty.

Table 2. Segment data for the Type-A faults. A segment is defined as one or more fault sections from the Fault Section Database (those composed of more than one have a "+" between the names in the "Sections in Segment" column). "DDW" stands for down-dip width and "Aseis Factor" is the effective area reduction due to aseismicity between the lower and upper seismogenic depths (those for N. San Andreas, Hayward-Rodgers Creek, and Calaveras represent a weight average of those listed in WGCEP-2002 Table 3.8). Area is the product of DDW, Length, and one minus the Aseis Factor. The slip rate and its standard deviation (σ_v) come from Deformation Model 2.1, and values that follow in parentheses are from Deformation Models 2.2 and 2.3, respectively (listed only if they differ from 2.1). All aforementioned values come from Appendix A, and those for segments composed of more than one section represent weight averages (weighted by area). "Event Rate" and its uncertainty (σ_λ) represent an estimate of the mean rate of events on a segment. These come from the Table 7 here (which ultimately comes from Table 7 of Appendix C), where multiple entries for a given segment have been combined here using a standard weight-average, and "NA" means no data are available. Finally, it's important to understand that slip rate and its uncertainty may be reduced in solving for final rates (via Equation Set (1)) depending on the values of the following parameters: "*Fract MoRate to Background*", "*Fraction Smaller Events & Aftershocks*", and "*Coupling Coefficient*".

Name	DDW (km)	Length (km)	Aseis Factor	Area (km^2)	Slip Rate, v (mm/yr)	σ_v (mm/yr)	Event Rate, λ (yr^{-1})	σ_λ (yr^{-1})	Sections in Segment
Elsinore									
W	14.6	46.2	0	674.8	2.5	0.5	5.195E-4	1.111E-3	Whittier, alt 2
GI	13.2	37.0	0	488.6	4.2	0.8	4.310E-3	5.444E-3	Glen Ivy, rev + Glen Ivy, stepover
T	14.2	51.8	0	734.9	4.4	0.9	5.429E-4	9.720E-4	Temecula, rev + Temecula, stepover
J	18.9	75.4	0	1426.1	5.0	1.0	5.391E-4	1.141E-3	Julian
CM	13.3	38.8	0	517.3	4.0	1.0	NA	NA	Coyote Mountain
Total		249.2		3841.7					
Garlock									
GE	11.5	45.2	0	519.3	3.0	1.0	NA	NA	Garlock (East)
GC	11.5	111.0	0	1276.1	7.0	1.0	6.238E-4	8.303E-4	Garlock (Central)
GW	14.7	97.6	0.1	1290.9	6.0	1.5	6.188E-4	8.681E-4	Garlock (West)
Total		253.7		3086.3					
San Jacinto									
SBV	16.1	45.1	0	725.7	6.0 (10.0, 3.0)	2.0 (4.0, 1.0)	NA	NA	San Bernardino
SJV	16.1	42.7	0	686.7	12.9 (15.8, 10.0)	2.5 (2.5, 2,5)	NA	NA	SJ Valley, rev + SJ Valley, stepover
A	16.8	71.1	0	1193.9	14.8 (18.1, 11.5)	2.8 (2.8, 2.8)	4.149E-3	2.316E-3	Anza, stepover + Anza, rev
C	16.8	46.8	0	786.1	14.0 (18.0, 10.0)	3.0 (3.0, 2.0)	NA	NA	Clark, rev
CC	15.9	42.9	0	681.5	4.0	3.0	NA	NA	Coyote Creek
B	13.1	34.2	0.1	403.6	4.0	3.0	NA	NA	Borrego

SM	12.4	26.3	0	325.8	5.0	1.5	1.812E-3	4.288E-3	Superstition Mtn
Total		309.0		4803.5					
S. San Andreas									
PK	10.2	36.4	0.79	78.0	34.0	2.5	NA	NA	Parkfield
CH	12.0	62.5	0	750.2	34.0	2.5	NA	NA	Cholame, rev
CC	15.1	59.0	0	891.2	34.0	1.5	4.101E-3	1.689E-3	Carrizo, rev
BB	15.1	49.7	0	751.0	34.0	1.5	NA	NA	Big Bend
NM	15.1	36.9	0	556.5	27.0	3.5	NA	NA	Mojave N
SM	13.1	97.6	0	1279.0	29.0	3.5	7.843E-3	2.270E-3	Mojave S
NSB	12.8	35.3	0	451.9	22.0 (18.0, 25.0)	3.0 (2.5,5.0)	4.545E-3	2.679E-3	San Bernardino N
SSB	12.8	43.4	0	555.5	16.0 (10.0, 16.0)	3.0 (3.0,4.0)	2.298E-3	2.117E-3	San Bernardino S
BG	15.1	55.9	0	843.0	10.0 (5.0,11.0)	3.0 (1.0, 3.0)	2.941E-3	2.108E-3	San Gorgonio Pass-Garnet HIll
CO	11.1	69.4	0.1	693.4	20.0 (16.0,24.0)	3.0 (3.0, 3.0)	3.125E-3	2.283E-3	Coachella, rev
Total		546.1		6849.7					
N. San Andreas									
SAO	11.0	136.1	0.02	1469.9	24.0	1.5	NA	NA	Offshore
SAN	11.0	189.4	0.02	2044.4	24.0	1.5	3.574E-3	1.972E-3	North Coast
SAP	13.0	84.5	0.02	1078.4	17.0	2.0	NA	NA	Peninsula
SAS	15.0	62.1	0.1	838.5	17.0	2.0	7.092E-3	6.481E-3	Santa Cruz Mtn
Total		472.1		5431.1					
Hayward-Rodgers Creek									
RC	12.0	62.4	0.02	734.5	9.0	1.0	NA	NA	Rodgers Creek
HN	12.0	34.8	0.4	250.7	9.0	1.0	2.915E-3	2.905E-3	Hayward (No)
HS	12.0	52.5	0.4	377.7	9.0	1.0	5.291E-3	4.085E-3	Hayward (So)
Total		149.6		1362.8					
Calaveras									
CN	13.0	45.2	0.2	470.2	6.0	1.0	1.252E-3	1.955E-3	Calaveras (No)
CC	11.0	58.9	0.76	155.5	15.0	1.5	NA	NA	Calaveras (Central)
CS	11.0	19.3	0.8	42.5	15.0	1.5	NA	NA	Calaveras (So)
Total		123.4		668.2					

Table 3. Rupture-model data for the seven Type-A faults. The rupture names represent the segments involved (see table 2 for segment definitions). "Ells-B" and "H&B" stand for Ellsworth-B and Hanks and Bakun magnitude-area relationships, respectively. The values under "Ells-B Rate" and "H&B Rate" are for the moment-balanced models described in the text (and using Deformation Model D2.1). "UCERF1 Mag" values represent the average magnitudes for the corresponding rupture in WGCEP UCERF 1 (Petersen et al., 2007), and "UCERF1 Rate" values represent the *total* rate of the associated ruptures (i.e., from the cumulative magnitude frequency distribution for the rupture). "NA" means no associated value exists in UCERF 1. See the text for more information on UCERF 1 rates and how they relate to other previous models (*e.g.*, WGCEP-2002 and NSHMP-2002).

	Rupture Name (segments involved)	Area (km^2)	Ells-B Mag	H&B Mag	A-Priori Rate	Ells-B Rate	H&B Rate	UCERF1 Rate	UCERF1 Mag
Elsinore									
1	W	674.8	7.03	6.84	7.14E-04	9.27E-04	1.37E-03	1.64E-03	6.80
2	GI	488.6	6.89	6.67	2.55E-03	1.19E-03	2.19E-03	3.09E-03	6.80
3	T	734.9	7.07	6.89	6.10E-04	1.24E-04	3.46E-04	4.38E-03	6.80
4	J	1426.1	7.35	7.28	Unlikely	3.85E-05	2.48E-05	3.09E-03	7.10
5	CM	517.3	6.91	6.69	5.71E-04	1.04E-03	2.11E-03	1.68E-03	6.80
6	W+GI	1163.4	7.27	7.16	Unlikely	2.48E-05	1.42E-04	0.00E+00	NA
7	GI+T	1223.5	7.29	7.19	8.90E-04	1.25E-04	1.25E-04	0.00E+00	NA
8	T+J	2161	7.53	7.52	Unknown	1.27E-04	1.26E-04	0.00E+00	NA
9	J+CM	1943.3	7.49	7.45	Unknown	1.74E-04	2.92E-04	0.00E+00	NA
10	W+GI+T	1898.3	7.48	7.44	Unlikely	2.48E-05	9.07E-05	0.00E+00	NA
11	GI+T+J	2649.6	7.62	7.63	Unknown	1.26E-04	1.27E-04	0.00E+00	NA
12	T+J+CM	2678.2	7.63	7.64	2.50E-04	2.83E-04	2.54E-04	0.00E+00	NA
13	W+GI+T+J	3324.4	7.72	7.77	Unlikely	2.52E-05	2.48E-05	0.00E+00	NA
14	GI+T+J+CM	3166.9	7.7	7.74	2.50E-04	1.83E-04	1.27E-04	0.00E+00	NA
15	W+GI+T+J+CM	3841.7	7.78	7.85	Unlikely	2.49E-05	2.52E-05	0.00E+00	NA
Total					*5.84E-3*	*4.43E-03*	*7.37E-03*	*1.39E-02*	
Garlock									
1	GE	519.3	6.92	6.7	6.80E-04	3.61E-04	6.21E-04	NA	NA
2	GC	1276.1	7.31	7.21	7.84E-05	9.26E-05	8.32E-05	NA	NA
3	GW	1290.9	7.31	7.22	2.36E-04	2.19E-04	2.61E-04	NA	NA
4	GE+GC	1795.4	7.45	7.41	7.84E-05	9.05E-05	8.32E-05	NA	NA
5	GC+GW	2567.1	7.61	7.62	3.13E-04	5.99E-04	5.50E-04	NA	NA
6	GE+GC+GW	3086.3	7.69	7.72	3.13E-04	5.83E-04	5.78E-04	NA	NA
Total					*1.70E-3*	*1.95E-03*	*2.18E-03*	*NA*	*NA*

San Jacinto									
1	SBV	725.7	7.06	6.88	2.31E-03	4.39E-04	4.42E-04	1.05E-02	6.70
2	SJV	686.7	7.04	6.85	2.43E-03	4.50E-04	4.49E-04	1.27E-02	6.90
3	A	1193.9	7.28	7.17	Unlikely	8.83E-05	8.82E-05	0.00E+00	NA
4	C	786.1	7.1	6.93	Unlikely	8.87E-05	8.98E-05	0.00E+00	NA
5	CC	681.5	7.03	6.85	8.89E-04	4.50E-04	4.48E-04	6.00E-03	6.80
6	B	403.6	6.81	6.59	4.82E-03	4.45E-04	4.43E-04	6.00E-03	6.60
7	SM	325.8	6.71	6.49	1.09E-03	1.50E-03	4.01E-03	2.10E-03	6.60
8	SBV+SJV	1412.4	7.35	7.27	1.32E-03	4.49E-04	4.41E-04	0.00E+00	NA
9	SJV+A	1880.6	7.47	7.44	Unknown	4.41E-04	4.50E-04	0.00E+00	NA
10	A+C	1980.1	7.5	7.47	3.15E-03	1.21E-03	1.16E-03	4.20E-03	7.20
11	A+CC	1875.4	7.47	7.43	Unlikely	8.82E-05	9.00E-05	0.00E+00	NA
12	CC+B	1085.1	7.24	7.12	8.89E-04	4.50E-04	4.47E-04	0.00E+00	NA
13	B+SM	729.4	7.06	6.89	1.09E-03	4.40E-04	4.43E-04	0.00E+00	NA
14	SBV+SJV+A	2606.4	7.62	7.62	Unknown	4.47E-04	4.48E-04	0.00E+00	NA
15	SJV+A+C	2666.8	7.63	7.64	Unknown	4.48E-04	4.51E-04	0.00E+00	NA
16	SJV+A+CC	2562.2	7.61	7.61	Unlikely	8.91E-05	8.93E-05	0.00E+00	NA
17	A+CC+B	2279.1	7.56	7.55	Unlikely	9.02E-05	8.95E-05	0.00E+00	NA
18	CC+B+SM	1411	7.35	7.27	8.89E-04	4.48E-04	4.40E-04	0.00E+00	NA
19	SBV+SJV+A+C	3392.5	7.73	7.78	1.05E-03	4.49E-04	4.41E-04	0.00E+00	NA
20	SBV+SJV+A+CC	3287.9	7.72	7.76	Unlikely	8.94E-05	9.03E-05	0.00E+00	NA
21	SJV+A+CC+B	2965.8	7.67	7.7	Unlikely	8.82E-05	8.89E-05	0.00E+00	NA
22	A+CC+B+SM	2604.9	7.62	7.62	Unlikely	8.93E-05	8.96E-05	0.00E+00	NA
23	SBV+SJV+A+CC+B	3691.5	7.77	7.83	Unlikely	8.80E-05	8.97E-05	0.00E+00	NA
24	SJV+A+CC+B+SM	3291.6	7.72	7.76	Unlikely	8.94E-05	9.03E-05	0.00E+00	NA
25	SBV+SJV+A+CC+B+SM	4017.3	7.8	7.88	Unlikely	8.90E-05	8.82E-05	0.00E+00	NA
Total					*1.99E-2*	*9.05E-03*	*1.15E-02*	*4.15E-02*	*NA*
N. San Andreas									
1	SAO	1469.9	7.37	7.29	4.93E-04	1.16E-03	1.01E-03	2.34E-04	7.29
2	SAN	2044.4	7.51	7.48	2.09E-05	2.00E-05	1.99E-05	1.48E-04	7.45
3	SAP	1078.4	7.23	7.11	5.31E-04	1.22E-04	1.05E-05	5.27E-04	7.15
4	SAS	838.5	7.12	6.97	7.64E-04	2.09E-03	2.40E-03	7.58E-04	7.03
5	SAO+SAN	3514.3	7.75	7.80	1.07E-03	2.77E-03	2.99E-03	1.31E-03	7.70
6	SAN+SAP	3122.8	7.69	7.73	Unlikely	2.08E-06	2.11E-06	0.00E+00	7.65
7	SAP+SAS	1916.9	7.48	7.45	1.03E-03	2.19E-03	3.63E-03	1.03E-03	7.42
8	SAO+SAN+SAP	4592.7	7.86	7.95	8.21E-05	7.10E-05	4.91E-05	8.15E-05	7.83

9	SAN+SAP+SAS	3961.3	7.80	7.87	2.52E-05	2.32E-05	2.27E-05	2.50E-05	7.76
10	SAO+SAN+SAP+SAS	5431.1	7.93	8.05	2.84E-03	9.97E-04	3.09E-04	2.81E-03	7.90
Total					*6.85E-3*	*9.45E-03*	*1.05E-02*		
S. San Andreas									
1	PK	78	6.09	5.87	3.46E-02	2.49E-02	5.26E-02	NA	NA
2	CH	750.2	7.08	6.9	5.00E-05	5.21E-05	5.46E-05	NA	NA
3	CC	891.2	7.15	7	3.00E-04	1.60E-04	5.74E-05	NA	NA
4	BB	751	7.08	6.9	3.00E-04	5.68E-04	5.26E-04	NA	NA
5	NM	556.5	6.95	6.73	2.00E-04	1.05E-04	1.44E-04	NA	NA
6	SM	1279	7.31	7.21	5.00E-04	6.45E-04	6.78E-04	NA	NA
7	NSB	451.9	6.86	6.64	7.00E-04	7.12E-04	6.64E-04	NA	NA
8	SSB	555.5	6.94	6.73	5.00E-05	5.10E-05	5.17E-05	NA	NA
9	BG	843	7.13	6.97	5.00E-04	1.88E-04	1.35E-05	NA	NA
10	CO	693.4	7.04	6.86	2.50E-03	6.70E-03	1.21E-02	NA	NA
11	PK+CH	828.2	7.12	6.96	1.60E-03	4.36E-03	7.01E-03	NA	NA
12	CH+CC	1641.4	7.42	7.36	3.00E-04	2.39E-04	2.15E-04	NA	NA
13	CC+BB	1642.2	7.42	7.36	Unknown	5.02E-06	5.07E-06	NA	NA
14	BB+NM	1307.5	7.32	7.23	Unlikely	1.01E-06	1.01E-06	NA	NA
15	NM+SM	1835.4	7.46	7.42	7.00E-04	4.95E-06	5.04E-06	NA	NA
16	SM+NSB	1730.9	7.44	7.39	6.00E-04	8.79E-04	8.90E-04	NA	NA
17	NSB+SSB	1007.4	7.2	7.07	8.00E-04	1.05E-03	1.22E-03	NA	NA
18	SSB+BG	1398.5	7.35	7.26	9.00E-04	5.03E-06	4.95E-06	NA	NA
19	BG+CO	1536.4	7.39	7.32	7.00E-04	2.83E-04	4.10E-04	NA	NA
20	PK+CH+CC	1719.4	7.44	7.38	7.00E-04	4.26E-04	4.19E-04	NA	NA
21	CH+CC+BB	2392.4	7.58	7.58	Unlikely	9.94E-07	9.93E-07	NA	NA
22	CC+BB+NM	2198.7	7.54	7.53	Unlikely	1.00E-06	1.01E-06	NA	NA
23	BB+NM+SM	2586.4	7.61	7.62	2.50E-04	1.88E-04	2.67E-04	NA	NA
24	NM+SM+NSB	2287.4	7.56	7.55	1.00E-04	7.24E-05	6.69E-05	NA	NA
25	SM+NSB+SSB	2286.4	7.56	7.55	4.00E-04	6.05E-04	7.55E-04	NA	NA
26	NSB+SSB+BG	1850.4	7.47	7.43	4.00E-04	2.22E-04	3.05E-05	NA	NA
27	SSB+BG+CO	2091.9	7.52	7.5	4.00E-04	2.23E-04	2.48E-04	NA	NA
28	PK+CH+CC+BB	2470.4	7.59	7.59	4.00E-04	8.20E-04	8.34E-04	NA	NA
29	CH+CC+BB+NM	2948.8	7.67	7.7	Unlikely	9.91E-07	9.99E-07	NA	NA
30	CC+BB+NM+SM	3477.7	7.74	7.79	4.00E-04	1.95E-04	4.99E-06	NA	NA
31	BB+NM+SM+NSB	3038.4	7.68	7.71	Unlikely	9.95E-07	1.00E-06	NA	NA
32	NM+SM+NSB+SSB	2842.9	7.65	7.68	2.00E-04	1.04E-04	1.02E-04	NA	NA

33	SM+NSB+SSB+BG	3129.4	7.7	7.73	3.00E-04	2.92E-04	1.97E-04	NA	NA
34	NSB+SSB+BG+CO	2543.8	7.61	7.61	4.00E-04	2.23E-04	2.17E-04	NA	NA
35	PK+CH+CC+BB+NM	3026.9	7.68	7.71	7.00E-04	1.54E-03	1.66E-03	NA	NA
36	CH+CC+BB+NM+SM	4227.8	7.83	7.9	5.00E-04	4.16E-04	2.67E-04	NA	NA
37	CC+BB+NM+SM+NSB	3929.6	7.79	7.86	1.00E-04	8.64E-05	5.55E-05	NA	NA
38	BB+NM+SM+NSB+SSB	3593.9	7.76	7.81	5.00E-05	4.92E-05	5.42E-05	NA	NA
39	NM+SM+NSB+SSB+BG	3685.9	7.77	7.83	1.00E-04	6.19E-05	3.29E-05	NA	NA
40	SM+NSB+SSB+BG+CO	3822.8	7.78	7.85	4.00E-04	3.58E-04	4.16E-04	NA	NA
41	PK+CH+CC+BB+NM+SM	4305.9	7.83	7.92	2.00E-03	1.04E-03	6.43E-04	NA	NA
42	CH+CC+BB+NM+SM+NSB	4679.8	7.87	7.96	Unlikely	9.91E-07	9.89E-07	NA	NA
43	CC+BB+NM+SM+NSB+SSB	4485.1	7.85	7.94	1.00E-04	9.04E-05	6.76E-05	NA	NA
44	BB+NM+SM+NSB+SSB+BG	4436.9	7.85	7.93	Unlikely	1.01E-06	1.01E-06	NA	NA
45	NM+SM+NSB+SSB+BG+CO	4379.2	7.84	7.93	1.00E-04	6.01E-05	3.90E-05	NA	NA
46	PK+CH+CC+BB+NM+SM+NSB	4757.8	7.88	7.97	5.00E-04	4.21E-04	3.49E-04	NA	NA
47	CH+CC+BB+NM+SM+NSB+SSB	5235.3	7.92	8.03	5.00E-05	5.00E-05	5.09E-05	NA	NA
48	CC+BB+NM+SM+NSB+SSB+BG	5328.1	7.93	8.04	5.00E-05	4.44E-05	3.00E-05	NA	NA
49	BB+NM+SM+NSB+SSB+BG+CO	5130.2	7.91	8.02	5.00E-05	4.50E-05	4.70E-05	NA	NA
50	PK+CH+CC+BB+NM+SM+NSB+SSB	5313.3	7.93	8.04	1.00E-04	1.00E-04	1.09E-04	NA	NA
51	CH+CC+BB+NM+SM+NSB+SSB+BG	6078.2	7.98	8.12	Unlikely	9.95E-07	1.01E-06	NA	NA
52	CC+BB+NM+SM+NSB+SSB+BG+CO	6021.5	7.98	8.11	1.00E-05	9.66E-06	9.24E-06	NA	NA
53	PK+CH+CC+BB+NM+SM+NSB+SSB+BG	6156.3	7.99	8.12	5.00E-05	4.65E-05	4.09E-05	NA	NA
54	CH+CC+BB+NM+SM+NSB+SSB+BG+CO	6771.6	8.03	8.18	Unlikely	1.01E-06	9.93E-07	NA	NA
55	PK+CH+CC+BB+NM+SM+NSB+SSB+BG+CO	6849.7	8.04	8.18	1.00E-04	8.29E-05	6.59E-05	NA	NA
Total					*5.42E-2*	*4.88E-02*	*8.37E-02*	*NA*	*NA*
Hayward-Rogers Creek									
1	RC	734.5	7.07	6.89	4.36E-03	2.69E-03	5.21E-03	4.26E-03	6.98
2	HN	250.7	6.60	6.38	3.48E-03	2.73E-03	4.27E-03	3.40E-03	6.49
3	HS	377.7	6.78	6.56	3.72E-03	2.86E-03	4.59E-03	3.64E-03	6.67
4	RC+HN	985.2	7.19	7.06	5.22E-04	4.67E-04	5.68E-04	5.10E-04	7.11
5	HN+HS	628.3	7.00	6.80	2.64E-03	1.43E-03	3.97E-03	2.58E-03	6.91
6	RC+HN+HS	1362.8	7.33	7.25	3.09E-04	2.75E-04	3.62E-04	3.02E-04	7.26
Total					*1.50E-2*	*1.05E-02*	*1.90E-02*		
Calaveras									
1	CN	470.2	6.87	6.65	1.03E-03	1.29E-03	2.31E-03	3.74E-03	6.78
2	CC	155.5	6.39	6.17	7.66E-03	6.82E-03	1.45E-02	5.78E-03	6.23
3	CS	42.5	5.83	5.61	1.05E-02	1.98E-02	4.25E-02	7.93E-03	5.79

4	CN+CC	625.7	7	6.8	1.29E-04	1.34E-04	1.58E-04	9.70E-05	6.90
5	CC+CS	198	6.5	6.28	2.60E-03	3.28E-03	6.32E-03	1.96E-03	6.36
6	CN+CC+CS	668.2	7.02	6.84	9.07E-04	1.25E-03	2.85E-03	6.84E-04	6.93
Total					*2.28E-2*	*3.26E-02*	*6.86E-02*		

Table 4. Segment event rates (per year) for the A-priori models and the two moment balanced models. "Ells-B" and "H&B" stand for Ellsworth-B and Hanks and Bakun magnitude-area relationships, respectively. The values under "Ells-B Rate" and "H&B Rate" are for the moment-balanced models described in the text (and using Deformation Model D2.1).

	Segment Name	A-Priori Rate	Ells-B Rate	H&B Rate
Elsinore				
1	W	7.143E-4	1.027E-3	1.656E-3
2	GI	3.690E-3	1.719E-3	2.852E-3
3	T	2.000E-3	1.042E-3	1.244E-3
4	J	5.000E-4	9.809E-4	9.996E-4
5	CM	1.071E-3	1.702E-3	2.803E-3
Garlock				
1	GE	1.071E-3	1.034E-3	1.282E-3
2	GC	7.837E-4	1.365E-3	1.294E-3
3	GW	8.628E-4	1.401E-3	1.389E-3
San Jacinto				
1	SBV	4.684E-3	2.050E-3	2.040E-3
2	SJV	4.800E-3	3.217E-3	3.216E-3
3	A	4.193E-3	3.881E-3	3.844E-3
4	C	4.193E-3	2.193E-3	2.142E-3
5	CC	2.667E-3	2.149E-3	2.141E-3
6	B	7.692E-3	2.317E-3	2.309E-3
7	SM	3.077E-3	2.660E-3	5.165E-3
N. San Andreas				
1	SAO	4.479E-3	5.001E-3	4.358E-3
2	SAN	4.032E-3	3.884E-3	3.389E-3
3	SAP	4.509E-3	3.406E-3	4.027E-3
4	SAS	4.660E-3	5.305E-3	6.365E-3
S. San Andreas				
1	PK	4.075E-2	3.377E-2	6.371E-2

2	CH	7.050E-3	9.597E-3	1.172E-2
3	CC	6.360E-3	5.773E-3	4.889E-3
4	BB	5.710E-3	5.803E-3	5.095E-3
5	NM	6.410E-3	4.816E-3	4.119E-3
6	SM	7.710E-3	5.949E-3	5.249E-3
7	NSB	5.660E-3	5.667E-3	5.518E-3
8	SSB	5.010E-3	3.773E-3	3.795E-3
9	BG	4.460E-3	2.147E-3	1.805E-3
10	CO	4.660E-3	7.982E-3	1.355E-2
Hayward-Rogers Creek				
1	RC	5.191E-3	3.436E-3	6.142E-3
2	HN	6.952E-3	4.897E-3	9.169E-3
3	HS	6.668E-3	4.563E-3	8.919E-3
Calaveras				
1	CN	2.066E-3	2.673E-3	5.317E-3
2	CC	1.130E-2	1.148E-2	2.385E-2
3	CS	1.402E-2	2.435E-2	5.162E-2

Table 5. Rupture rates for Moment Balanced models using Deformation Models D2.2 and D2.3 and the alternative magnitude-area relationships. "Ells-B" and "H&B" stand for the Ellsworth-B and Hanks and Bakun magnitude-area relationships, respectively.

		D2.2		D2.3	
	Rupture Name (segments involved)	**Ells-B Rate**	**H&B Rate**	**Ells-B Rate**	**H&B Rate**
San Jacinto		1.57E-03	2.30E-03	4.39E-04	4.42E-04
1	SBV	1.23E-03	1.41E-03	4.50E-04	4.49E-04
2	SJV	8.83E-05	8.82E-05	8.83E-05	8.82E-05
3	A	8.87E-05	8.98E-05	8.87E-05	8.98E-05
4	C	4.50E-04	4.48E-04	4.50E-04	4.48E-04
5	CC	4.45E-04	4.43E-04	4.45E-04	4.43E-04
6	B	1.50E-03	4.01E-03	1.50E-03	4.01E-03
7	SM	4.86E-04	7.08E-04	4.49E-04	4.41E-04
8	SBV+SJV	4.41E-04	4.50E-04	4.41E-04	4.50E-04
9	SJV+A	2.11E-03	2.15E-03	7.95E-04	7.36E-04
10	A+C	8.82E-05	9.00E-05	8.82E-05	9.00E-05
11	A+CC	4.50E-04	4.47E-04	4.50E-04	4.47E-04
12	CC+B	4.40E-04	4.43E-04	4.40E-04	4.43E-04
13	B+SM	4.47E-04	4.48E-04	4.47E-04	4.48E-04
14	SBV+SJV+A	4.48E-04	4.51E-04	4.48E-04	4.51E-04
15	SJV+A+C	8.91E-05	8.93E-05	8.91E-05	8.93E-05
16	SJV+A+CC	9.02E-05	8.95E-05	9.02E-05	8.95E-05
17	A+CC+B	4.48E-04	4.40E-04	4.48E-04	4.40E-04
18	CC+B+SM	4.49E-04	4.41E-04	4.49E-04	4.41E-04
19	SBV+SJV+A+C	8.94E-05	9.03E-05	8.94E-05	9.03E-05
20	SBV+SJV+A+CC	8.82E-05	8.89E-05	8.82E-05	8.89E-05
21	SJV+A+CC+B	8.93E-05	8.96E-05	8.93E-05	8.96E-05
22	A+CC+B+SM	8.80E-05	8.97E-05	8.80E-05	8.97E-05
23	SBV+SJV+A+CC+B	8.94E-05	9.03E-05	8.94E-05	9.03E-05
24	SJV+A+CC+B+SM	8.90E-05	8.82E-05	8.90E-05	8.82E-05
25	SBV+SJV+A+CC+B+SM	1.19E-02	1.56E-02	8.63E-03	1.11E-02
Total		*1.57E-03*	*2.30E-03*	*4.39E-04*	*4.42E-04*
S. San Andreas					
1	PK	2.49E-02	5.26E-02	2.49E-02	5.18E-02
2	CH	5.21E-05	5.46E-05	5.21E-05	5.47E-05

3	CC	1.61E-04	5.86E-05	1.57E-04	5.49E-05
4	BB	5.74E-04	5.37E-04	5.57E-04	5.13E-04
5	NM	9.46E-05	1.32E-04	1.27E-04	1.61E-04
6	SM	7.64E-04	8.62E-04	3.78E-04	3.71E-04
7	NSB	7.09E-04	6.40E-04	1.33E-03	1.09E-03
8	SSB	4.98E-05	5.09E-05	4.79E-05	4.96E-05
9	BG	1.72E-04	4.35E-05	2.85E-04	6.21E-05
10	CO	6.02E-03	1.10E-02	7.97E-03	1.44E-02
11	PK+CH	4.36E-03	6.99E-03	4.37E-03	7.06E-03
12	CH+CC	2.41E-04	2.16E-04	2.36E-04	2.14E-04
13	CC+BB	5.02E-06	5.07E-06	5.02E-06	5.07E-06
14	BB+NM	1.01E-06	1.01E-06	1.01E-06	1.01E-06
15	NM+SM	4.95E-06	5.04E-06	4.95E-06	5.04E-06
16	SM+NSB	1.10E-03	1.23E-03	1.03E-03	1.02E-03
17	NSB+SSB	6.38E-04	7.83E-04	1.17E-03	1.36E-03
18	SSB+BG	5.03E-06	4.95E-06	5.03E-06	4.95E-06
19	BG+CO	1.65E-04	3.45E-04	6.88E-04	9.59E-04
20	PK+CH+CC	4.36E-04	4.25E-04	4.07E-04	4.16E-04
21	CH+CC+BB	9.94E-07	9.93E-07	9.94E-07	9.93E-07
22	CC+BB+NM	1.00E-06	1.01E-06	1.00E-06	1.01E-06
23	BB+NM+SM	1.90E-04	2.69E-04	1.78E-04	2.42E-04
24	NM+SM+NSB	7.60E-05	7.20E-05	8.15E-05	7.82E-05
25	SM+NSB+SSB	6.04E-04	7.82E-04	6.30E-04	7.66E-04
26	NSB+SSB+BG	3.62E-05	5.04E-06	1.76E-04	5.04E-06
27	SSB+BG+CO	5.83E-05	8.01E-05	7.86E-05	7.99E-05
28	PK+CH+CC+BB	8.40E-04	8.87E-04	7.81E-04	7.66E-04
29	CH+CC+BB+NM	9.91E-07	9.99E-07	9.91E-07	9.99E-07
30	CC+BB+NM+SM	1.98E-04	4.99E-06	1.75E-04	4.99E-06
31	BB+NM+SM+NSB	9.95E-07	1.00E-06	9.95E-07	1.00E-06
32	NM+SM+NSB+SSB	9.53E-05	8.57E-05	1.33E-04	1.42E-04
33	SM+NSB+SSB+BG	2.24E-04	1.43E-04	2.61E-04	1.04E-04
34	NSB+SSB+BG+CO	5.01E-06	5.02E-06	2.44E-04	2.75E-04
35	PK+CH+CC+BB+NM	1.45E-03	1.47E-03	1.73E-03	1.95E-03
36	CH+CC+BB+NM+SM	4.18E-04	2.72E-04	3.90E-04	1.58E-04
37	CC+BB+NM+SM+NSB	8.83E-05	5.90E-05	9.74E-05	7.20E-05
38	BB+NM+SM+NSB+SSB	4.84E-05	5.24E-05	5.19E-05	5.83E-05

39	NM+SM+NSB+SSB+BG	5.20E-05	1.89E-05	6.43E-05	3.27E-05
40	SM+NSB+SSB+BG+CO	1.69E-04	1.93E-04	3.60E-04	4.01E-04
41	PK+CH+CC+BB+NM+SM	1.07E-03	7.14E-04	6.24E-04	5.02E-06
42	CH+CC+BB+NM+SM+NSB	9.91E-07	9.89E-07	9.91E-07	9.89E-07
43	CC+BB+NM+SM+NSB+SSB	8.72E-05	6.03E-05	1.02E-04	8.68E-05
44	BB+NM+SM+NSB+SSB+BG	1.01E-06	1.01E-06	1.01E-06	1.01E-06
45	NM+SM+NSB+SSB+BG+CO	4.55E-05	1.54E-05	6.63E-05	5.01E-05
46	PK+CH+CC+BB+NM+SM+NSB	4.68E-04	4.41E-04	6.84E-04	7.92E-04
47	CH+CC+BB+NM+SM+NSB+SSB	4.92E-05	4.89E-05	5.30E-05	5.64E-05
48	CC+BB+NM+SM+NSB+SSB+BG	4.16E-05	2.49E-05	4.60E-05	3.14E-05
49	BB+NM+SM+NSB+SSB+BG+CO	4.10E-05	3.99E-05	4.73E-05	5.13E-05
50	PK+CH+CC+BB+NM+SM+NSB+SSB	9.74E-05	1.01E-04	1.13E-04	1.32E-04
51	CH+CC+BB+NM+SM+NSB+SSB+BG	9.95E-07	1.01E-06	9.95E-07	1.01E-06
52	CC+BB+NM+SM+NSB+SSB+BG+CO	9.50E-06	8.93E-06	9.76E-06	9.43E-06
53	PK+CH+CC+BB+NM+SM+NSB+SSB+BG	4.37E-05	3.54E-05	4.82E-05	4.28E-05
54	CH+CC+BB+NM+SM+NSB+SSB+BG+CO	1.01E-06	9.93E-07	1.01E-06	9.93E-07
55	PK+CH+CC+BB+NM+SM+NSB+SSB+BG+CO	6.64E-05	3.26E-05	9.39E-05	8.73E-05
Total		*4.71E-02*	*8.19E-02*	*5.10E-02*	*8.60E-02*

Table 6. Segment rates for Moment Balanced models using Deformation Models D2.2 and D2.3 and the alternative magnitude-area relationships. "Ells-B" and "H&B" stand for the Ellsworth-B and Hanks and Bakun magnitude-area relationships, respectively.

		D2.2		D2.2	
	Segment Name	Ells-B Rate	H&B Rate	Ells-B Rate	H&B Rate
San Jacinto		3.22E-03	4.16E-03	2.05E-03	2.04E-03
1	SBV	4.03E-03	4.45E-03	3.22E-03	3.22E-03
2	SJV	4.78E-03	4.84E-03	3.47E-03	3.42E-03
3	A	3.09E-03	3.14E-03	1.78E-03	1.72E-03
4	C	2.15E-03	2.14E-03	2.15E-03	2.14E-03
5	CC	2.32E-03	2.31E-03	2.32E-03	2.31E-03
6	B	2.66E-03	5.17E-03	2.66E-03	5.17E-03
7	SM	3.22E-03	4.16E-03	2.05E-03	2.04E-03
S. San Andreas					
1	PK	3.38E-02	6.37E-02	3.37E-02	6.30E-02
2	CH	9.60E-03	1.17E-02	9.59E-03	1.17E-02
3	CC	5.78E-03	4.88E-03	5.76E-03	4.89E-03
4	BB	5.79E-03	5.08E-03	5.80E-03	5.07E-03
5	NM	4.74E-03	3.98E-03	4.93E-03	4.26E-03
6	SM	6.06E-03	5.58E-03	5.73E-03	4.80E-03
7	NSB	4.80E-03	4.89E-03	6.90E-03	6.74E-03
8	SSB	2.47E-03	2.57E-03	3.80E-03	3.83E-03
9	BG	1.14E-03	9.98E-04	2.48E-03	2.20E-03
10	CO	6.58E-03	1.17E-02	9.56E-03	1.63E-02

Table 7. Paleoseismic event-rate data from Tables 7 of Appendix C. The fourth column here gives the association of each site with the segments defined in Table 2. The "Ells-B Pred" and "H & B Pred" columns represents the rates predicted by the unsegmented model for the Ellsworth-B and Hanks and Bakun magnitude-area relationships, respectively (and note that these are not total rates, but rather rates of visible ruptures, which were computed by multiplying the rate for each magnitude at each site by the probability of surface rupturing for that magnitude (from Youngs et al. (2003)). Values in red and blue are above and below, respectively, the 95%-confidence bounds for the observed Poisson rates. Only Deformation Model 2.1 has been applied here.

Site	Lat	Lon	Seg Num (Name)	Poisson Rate	rate sigma (Poisson)	2.5%	97.5%	Ells-B Pred	H & B Pred
Calaveras fault - North	37.5104	-121.8346	1 (CN)	0.001252	0.001955	0.000439	0.004348	5.68E-03	9.99E-03
Elsinore - Glen Ivy	33.7701	-117.4909	2 (GI)	0.004310	0.005444	0.001613	0.012500	1.27E-03	1.41E-03
Elsinore Fault - Julian	33.2071	-116.7273	4 (J)	0.000539	0.001141	0.000219	0.002500	1.50E-03	1.72E-03
Elsinore - Temecula	33.4100	-117.0400	3 (T)	0.000543	0.000972	0.000230	0.002174	1.58E-03	1.83E-03
Elsinore - Whittier	33.9303	-117.8437	1 (W)	0.000519	0.001111	0.000217	0.002439	6.91E-04	6.62E-04
Garlock - Central	35.4441	-117.6815	2 (GC)	0.000624	0.000830	0.000262	0.001923	2.36E-03	2.81E-03
Garlock - Western	34.9868	-118.5080	3 (GW)	0.000619	0.000868	0.000264	0.002000	1.49E-03	1.67E-03
Hayward fault - North	37.9306	-122.2977	2 (HN)	0.002915	0.002905	0.001333	0.007143	5.27E-03	8.29E-03
Hayward fault - South	37.5563	-121.9739	3 (HS)	0.005291	0.004085	0.002941	0.011111	2.12E-03	3.25E-03
N. San Andreas - Vendanta	38.0320	-122.7891	2 (SAN)	0.004237	0.002400	0.002193	0.007407	6.73E-03	6.07E-03
SAF - Arano Flat	36.9415	-121.6729	4 (SAS)	0.007092	0.006481	0.003704	0.016667	1.45E-03	1.21E-03
N. San Andreas - Fort Ross	38.5200	-123.2400	2 (SAN)	0.002193	0.003462	0.000769	0.007692	7.01E-03	6.38E-03
San Jacinto - Hog Lake	33.6153	-116.7091	3 (A)	0.004149	0.002316	0.002273	0.006993	5.20E-03	6.19E-03
San Jacinto - Superstition	32.9975	-115.9436	7 (SM)	0.001812	0.004288	0.000515	0.009091	1.93E-03	2.55E-03
San Andreas – Burro Flats	33.9730	-116.8170	8 (SSB)	0.002381	0.002494	0.002174	0.011111	5.83E-03	4.24E-03
SAF- Carrizo Bidart	35.2328	-119.7872	3 (CC)	0.005882	0.003529	0.001282	0.020000	5.32E-03	3.84E-03
SAF - Combined Carrizo Plain	35.1540	-119.7000	3 (CC)	0.003571	0.001924	0.001235	0.008333	5.66E-03	4.10E-03
San Andrteas - Indio	33.7414	-116.1870	10 (CO)	0.003125	0.002328	0.000855	0.011111	3.33E-03	2.66E-03
San Andreas - Pallett Creek	34.4556	-117.8870	6 (SM)	0.007353	0.002495	0.003534	0.013514	7.51E-03	5.37E-03
San Andreas - Pitman	34.2544	-117.4340	7 (NSB)	0.004545	0.002679	0.002273	0.012500	7.08E-03	5.08E-03

Canyon									
San Andreas - Plunge Creek	34.1158	-117.1370	8 (SSB)	0.002083	0.004005	0.000676	0.012500	6.53E-03	4.71E-03
Mission Creek - 1000 Palms	33.8200	-116.3010	9 (BG)	0.002941	0.002108	0.001075	0.010000	3.96E-03	3.04E-03
San Andreas - Wrightwood	34.3697	-117.6680	6 (SM)	0.010204	0.005476	0.005714	0.016667	7.39E-03	5.26E-03

Table 8. Parameters for the unsegmented models for each fault, where the San Jacinto fault has been separated into two different sources due to a branch on the fault. The Total Length, Area, and Moment Rate on the Elsinore differ from values listed in Table 2 because an overlapping fault section has been removed here (which is true also for the "San Jacinto (SB to C)" source as well). Ave Slip Rate and Aseismicity values are weighted averages, where the weights are fault-section area. Total Area and Moment Rate have been reduced according the value of Ave Aseismicity. Total moment rates listed here have also been reduced by 10% (relative to that computed from Ave Slip Rate and Total Area) according to the preferred values of "*Fract MoRate to Background*", "*Fraction Smaller Events & Aftershocks*", and "*Coupling Coefficient*" (see Table 1).

Fault Name	Ellsworth-B Magnitude	Hanks & Bakun Magnitude	Ellsworth-B Total Rate (M≥6.5)	Hanks & Bakun Total Rate (M≥6.5)	Ave Slip Rate (mm/yr)	Total Area	Total Length (km)	Total Moment Rate	Ave Aseismicity
Deformation Model D2.1:									
Calaveras	7.0	6.8	0.0093	0.0142	8.67	668.2	123.4	1.56E+17	0.65
Elsinore	7.8	7.8	0.0036	0.0036	4.40	3688.1	238.1	4.38E+17	0.00
Garlock	7.7	7.7	0.0052	0.0052	5.91	3086.3	253.7	4.92E+17	0.05
Hayward-Rogers Creek	7.3	7.2	0.0098	0.0125	9.00	1362.8	149.6	3.31E+17	0.24
N. San Andreas	7.9	8.0	0.0195	0.0147	21.53	5431.1	472.1	3.16E+18	0.03
S. San Andreas	8.0	8.2	0.0223	0.0126	25.88	6849.7	546.1	4.79E+18	0.06
San Jacinto (CC to SM)	7.3	7.3	0.0048	0.0048	4.23	1411.0	103.4	1.61E+17	0.03
San Jacinto (SB to C)	7.7	7.7	0.0121	0.0121	14.04	2990.9	181.2	1.13E+18	0.00
Deformation Model D2.2:									
S. San Andreas	8.0	8.2	0.0208	0.0118	24.10	6849.7	546.1	4.46E+18	0.06
San Jacinto (CC to SM)	7.3	7.3	0.0048	0.0048	4.23	1411.0	103.4	1.61E+17	0.03
San Jacinto (SB to C)	7.7	7.7	0.0155	0.0155	18.04	2990.9	181.2	1.46E+18	0.00
Deformation Model D2.3:									
S. San Andreas	8.0	8.2	0.0230	0.0130	26.60	6849.7	546.1	4.92E+18	0.06
San Jacinto (CC to SM)	7.3	7.3	0.0048	0.0048	4.23	1411.0	103.4	1.61E+17	0.03
San Jacinto (SB to C)	7.7	7.7	0.0088	0.0088	10.28	2990.9	181.2	8.30E+17	0.00